A central role for cAMP/EPAC/RAP/PI3K/AKT/CREB signaling in LH-induced follicular Pgr expression at medaka ovulation

Katsueki Ogiwara*, Miyuki Hoyagi, and Takayuki Takahashi

Laboratory of Reproductive and Developmental Biology, Faculty of Science, Hokkaido University, Sapporo 060–0810, Japan

***Corresponding author:**
Katsueki Ogiwara, Laboratory of Reproductive and Developmental Biology, Faculty of Science, Hokkaido University, Sapporo 060–0810, Japan
Tel.: 81–11–706–2748
Fax: 81–11–706–3522
E-mail: kogi@sci.hokudai.ac.jp

Running title: A signaling cascade for medaka Pgr induction.

Summary sentence: EPAC/RAP/PI3K/AKT/CREB signaling mediates LH-induced cAMP signaling to induce medaka Pgr expression in ovulating follicles.

Keywords: teleost, medaka, LH, ovulation, PGR, EPAC/RAP/PI3K/AKT/CREB signaling

Grant support: This work was supported by Grants-in-Aid for Scientific Research (16H04810 to T.T. and 23687009 to K.O.) from the Ministry of Education, Culture, Sports, Science and Technology of Japan.

Abstract

Nuclear progestin receptor (PGR) is a ligand-activated transcription factor that has been identified as a pivotal mediator of many processes associated with ovarian and uterine function, and aberrant control of PGR activity causes infertility and disease including cancer. The essential role of PGR in vertebrate ovulation is well recognized, but the mechanisms by which PGR is rapidly and transiently induced in preovulatory follicles after the ovulatory LH surge are not known in lower vertebrates. To address this issue, we utilized the small freshwater teleost medaka *Oryzias latipes*, which serves as a good model system for studying vertebrate ovulation. In the *in vitro* ovulation system using preovulatory follicles dissected from the fish ovaries, we found that inhibitors of EPAC (brefeldin A), RAP (GGTI298), PI3K (Wortmannin), AKT (AKT inhibitor IV), and CREB (KG-501) inhibited LH-induced follicle ovulation, while the PKA inhibitor H-89 had no effect on follicle ovulation. The inhibitors capable of inhibiting follicle ovulation also inhibited follicular expression of Pgr and matrix metalloproteinase-15 (Mmp15), the latter of which was previously shown to not only be a downstream effector of Pgr but also a proteolytic enzyme indispensable for follicle rupture in medaka ovulation. Further detailed analysis revealed for the first time that the cAMP/EPAC/RAP/PI3K/AKT/CREB signaling pathway mediates the LH signal to induce Pgr expression in preovulatory follicles. Our data also showed that phosphorylated Creb1 is a transcription factor essential for *pgr* expression and that Creb1 phosphorylated by Akt1, rather than PKA, may be preferably used to induce *pgr* expression.

Introduction

Nuclear progestin receptor (PGR) is a progestin-activated transcription factor that is expressed primarily in female reproductive tissues, immune and neuronal systems [1-3]. PGR, which is luteinizing hormone (LH)-inducible, shows pleiotropic effects on reproductive processes, and therefore, aberrant control of PGR action can not only cause infertility but also results in various diseases associated with the organs, such as ovarian and uterine cancer and endometriosis [1, 4]. Thus, an understanding of precise role of PGR in normal function of the reproductive organs would be useful from a therapeutic point of view.

Investigations of PGR have been intensively carried out in relation to ovulation [1, 5-11]. Since PGR is transiently and rapidly induced in the granulosa cells of preovulatory follicles immediately after the LH surge and because it subsequently provokes the expression of many ovulation-related genes in the cells, studies to date on PGR have sought to either identify PGR-regulated genes/proteins or to unveil the mechanism and signaling pathway by which LH induces PGR. In the former studies, many genes/proteins have been documented to be expressed under the control of PGR expressed in the follicle that is destined for ovulation [7, 8, 12-17]. On the other hand, attaining an understanding of the signaling pathway and regulatory mechanism underlying PGR expression in LH-stimulated preovulatory follicles still remains a challenge. Nevertheless, accumulating evidence indicates that in the preovulatory follicle subjected to the ovulatory LH surge, cAMP signaling evoked as a result of LH receptor activation sequentially flows via protein kinase A (PKA), epidermal growth factor (EGF)-like factors/ EGF receptor,

ERK1/2 (also known as MAPK3/1) and inositol trisphosphate (IP3)/ diacylglycerol (DAG). PGR is presumed to be expressed downstream of these mediators [15, 18-23]. In addition, the requirement of nuclear receptor-interacting protein 1 (NRIP1) [24] and activation of the Gαq/11 pathway [25] has been reported for PGR expression. One report investigated the expression of PGR in granulosa cells using an intact PGR promoter, with a focus on the LH inducibility of PGR [26]. The study revealed that LH activates Sp1/Sp3 binding sites in the PGR proximal promoter, but the molecular mechanisms by which this activation occurs leaves unanswered questions.

In all vertebrates, the ovary is principally regulated by the hypothalamus-pituitary-gonadal axis [27, 28]; thus, the growth and proliferation of oogonia, their development to the oocyte stage, and their eventual release from the ovary are believed to be under similar endocrine control. These considerations, together with the general concept that there are very few differences between teleosts and mammals at the molecular level [29], have encouraged the use of teleost models to understand ovary physiology conserved across vertebrates. Teleosts have been valuable animal models for examining the effects of natural environmental changes [30-32]. It is also known that environmental contaminants affect LH signaling, resulting in disruption of fertility in the wild teleost population. To understand how such contaminants cause infertility in teleosts, elucidation of the LH signaling pathway is a necessary task.

In teleosts, Pgr has also emerged as an important transcription factor for ovulation [6, 7, 33-35]. Notably, recent studies using *pgr* knockout zebrafish have revealed that fish exhibit anovulation and infertility and that, as in mammals, the expression of many

ovulation-related genes is changed in KO fish compared with wild type fish [6]. Previous studies using a freshwater teleost medaka, which serves as a good model for ovulation study [36], have revealed that membrane-type 2 matrix metalloproteinase 2 (official name, Mmp15) is indispensable for follicle rupture during medaka ovulation and that its expression is drastically induced before ovulation in the pre- and/or peri-ovulatory follicles of the fish ovary under the control of Pgr [34, 36, 37]. In addition, follicular *pgr* expression was induced in an LH- and cAMP-dependent manner [33]. However, similar to mammals, little is known about the intracellular signaling pathways leading from the LH surge to *pgr*/Pgr expression in the ovarian follicles of the fish. With this in mind, we address the currently ill-defined problem of the LH-elicited signaling pathways that eventually lead to *pgr*/Pgr expression using a medaka model. Here, we report a novel finding that an exchange protein directly activated by cAMP (Epac, official name, Rapgef), which is a multidomain protein that functions as a cAMP-activated exchange factor for the small G-proteins Rap1 and Rap2 [38-41], acts as a direct downstream effector of cAMP increased in the granulosa cells of LH-stimulated preovulatory follicles. Further analysis revealed that Epac1 activated with cAMP activates Rap1, which subsequently activates the phosphatidylinositol 3-kinase (PI3K)/AKT pathway, followed by phosphorylation of the transcription factor Creb1 and eventually leading to *pgr* expression in the follicles. This signaling pathway that induces *pgr* expression in the teleost ovary is completely different from that currently presumed for mammalian species.

Materials and methods

Medaka culture and tissue preparation

128

129 Adult medaka (*Oryzias latipes*), strain himedaka (orange-red variety), were purchased
130 from a local dealer. The fish were maintained and acclimated to the artificial reproductive
131 conditions, as previously described [36]. Under the conditions, females usually ovulate
132 every day just before the onset of light. In the present study, the start of the light period
133 was set as ovulation hour 0. Preovulatory follicles destined to ovulate (≥1.0 mm,
134 postvitellogenic phase, stage IX-X) were isolated as previously described [37]. Separation
135 of follicle layers from follicles was performed as previously described [36]. The
136 experimental procedures used in the present study were approved by the Committee of
137 the Experimental Plants and Animals, Hokkaido University.

138

139 *In vitro* follicle culture and ovulation

140

141 *In vitro* follicle culture was performed as previously described [42]. An outline of the
142 experiments is shown in Figure 1A. Preovulatory follicles, that had not yet been exposed
143 to an endogenous LH surge, were isolated from two to four fish ovaries 22 h before
144 ovulation (-22 h-follicles), pooled, and then divided into control and test groups. The
145 follicles (approximately 20–25 follicles per group) were incubated at 26 °C in 90% M199
146 medium (pH 7.4) in the presence of medaka recombinant LH (rLh) (100 μg/ml) with or
147 without specific inhibitors. The chemicals used were N-(cis-2-phenyl-cyclopentyl)
148 azacyclotridecan-2-imine-hydrochloride (MDL 12330A) (1-50 μM) (Calbiochem/Merck
149 KGaA, Darmstadt, Germany), NKY80 (adenylyl Cyclase Type V Inhibitor) (1-200 μM)
150 (Cayman, Ann Arbor, MI), H-89 (1-200 μM) (Santa-Cruz, Dallas, TX), PKA inhibitor 14-

22 amide (1-50 μM) (Sigma-Aldrich, St. Louis, MO), brefeldin A (1-50 μM) (Sigma-Aldrich), EPAC 5376753 (1-100 μM) (Focus Biomolecules, Plymouth Meeting, PA), Wortmannin (1-50 μM) (Calbiochem/Merck), GGTI 298 (1-200 μM) (Sigma-Aldrich), LY294002 (1-20 μM) (Calbiochem/Merck), AKT inhibitor IV (1-50 μM) (Calbiochem/Merck), AKT inhibitor (1-200 μM) (Santa-Cruz), naphthol AS-E phosphate (KG-501) (1-20 μM) (Sigma-Aldrich), CBP-CREB interaction inhibitor (1-500 μM) (Calbiochem/Merck), 8-bromoadenosine 3', 5'-cyclic monophosphate (8-Br-cAMP) (1 μM) (Sigma-Aldrich), forskolin (1 μM) (Sigma-Aldrich), U0126 (25 μM) (Wako, Osaka, Japan), EGFR inhibitor (50 μM) (Cayman), Salirasib (20 μM) (Focus Biomolecules), and PKC inhibitor (100 μM) (Santa-Cruz). After incubation for 3 h, 12 h, or 30 h, the follicles were collected and used for experiments. The follicles that successfully ovulated were counted after incubation for 30 h and ovulation rates were calibrated. Medaka rLh was prepared as previously described [37].

Cloning

As the nucleotide sequence of medaka *epac1* is different from that currently available from the National Center of Biotechnology Information (NCBI) database [43], the gene was subjected to cDNA cloning. The sequence of the 5' unknown region was determined using rapid amplification of 5'-cDNA ends according to previously reported methods [44], except that total RNA purified from preovulatory follicles isolated from ovaries 1 h after ovulation was used. The primers used are given in Supplementary Information (Supplemental Table S1). To confirm the sequence of the full-length cDNA, RT-PCR was conducted using KOD Fx DNA polymerase (Toyobo, Osaka, Japan) with the follicle

cDNA. The primers used were Epac1 full-SS and Epac1 full-AS (Supplemental Table S1). The PCR products were phosphorylated, gel-purified, and ligated into a pBluescript SK vector (Agilent Technologies, Santa Clara, CA). The nucleotide sequence of the resulting vector, pBlu-Epac1, was confirmed by sequencing. The determined sequence was deposited into the DDBJ/GenBank/NCBI database [43] (accession number: LC541574).

Reverse-transcription (RT) and real-time polymerase chain reaction (PCR)

Total RNA was purified using Isogen (Nippongene, Tokyo, Japan) according to the manufacturer's instructions. Real-time RT-PCR (qRT-PCR) was conducted according to a method previously described [44]. Ovarian and/or follicular expression of the following gene transcripts were analyzed: three Epac genes (*rapgef3, rapfef4a, and rapgef4b*), eight Rap genes (*rapgap1a, rapgap1b1, rapgap1b2, rapgap2a1, rapgap2a2, rapgap2b1, rapgap2b2, and rapgap2c*), four Pi3k catalytic subunits (*pik3c2a*, *pik3c2b*, *pik3c2g*, and *pik3c3*), four Akt genes (*akt1, akt2a, akt2b, and akt3*), one mTor gene (*mtor*), one Pdk1 gene (*pdk1*), and two Creb genes (*creb1 and creb2*). The primer pairs used are given in Supplementary Information (Supplemental Table S1). For analysis, a KOD SYBR qPCR Mix (Toyobo) or a KAPA Fast qPCR Kit (Nippon Genetics Co., Ltd., Tokyo, Japan) was used. Eukaryotic translation elongation factor 1 alpha (*eef1a1)* was used as the reference gene to normalize the expression level of the target genes.

Antibody preparation

Recombinant proteins acting as antigens were produced using an *E. coli* expression system. The coding regions of medaka *epac1* and *creb1*, or the partial cording regions of *pik3c2a*, *pik3c2b*, and *pik3c2g* were amplified via PCR with KOD -Plus- Neo DNA polymerase (Toyobo, Tokyo, Japan) using ovary cDNA. The primer pairs used are given in Supplementary Information (Supplemental Table S1). The PCR products were phosphorylated, gel-purified, and ligated into a pET30a vector (Novagen, Madison, WI) previously digested with *Eco*RV. The nucleotide sequence was confirmed by sequencing. Expression and purification of the recombinant proteins [45], immunization of mice with the antigens [37], and antibody purification [46] were performed according to previously described methods. Anti-medaka Akt1 antibody was produced in rabbits by a custom antibody production service (Eurofins Genomics K. K., Tokyo, Japan). The amino acid sequence of the KLH-conjugated peptide used was NH_2-CDSERRPHFPQFSYSAS-COOH. Anti-medaka Mmp15 antibody [36], rat anti-medaka Pgr antibody [34], mouse anti-medaka Pgr antibody [34], and anti-medaka ribosomal protein L7 (Rpl7) antibody [42] were prepared as previously described. The other antibodies used were commercially available; Rap1 antibody (GeneTex Inc., Irvine, CA, GTX61875), AKT1 (phospho-Ser473) antibody (GeneTex, GTX61708) and phospho-CREB (S133) (87G3) rabbit mAB (Cell Signaling, Inc., Beverly, MA, 9198S). The specificity of the antibodies was examined by western blot analysis (Supplemental Figure 1).

Tissue extract preparation, immunoprecipitation (IP), and western blot analysis

Preovulatory follicles isolated from medaka ovaries were used directly or after *in vitro*

223 incubation with or without additives for the indicated period of time. Follicles (30 follicles
224 per sample) were sonicated in IP buffer (50 mM Tris-HCl (pH 8.0), 0.2 M NaCl, 0.1%
225 SDS, and 1% Triton X-100) containing 1 × Protease Inhibitor Cocktail (Wako Chemicals,
226 Osaka, Japan) and 1× Phosphatase Inhibitor Cocktail Solution I (Wako) for a few seconds.
227 The samples were then incubated at 4 °C for 2 h with gentle agitation and centrifuged at
228 15,000 × g for 10 min. The resultant supernatants were used for Western blot analysis or
229 IP. Follicle layer extract was prepared as previously described [36]. Protein concentration
230 was determined using a BCA kit (Thermo Fischer Scientific, San Jose, CA).
231
232 IP was performed as previously described [34] with a slight modification. Briefly, the
233 samples (3 mg each) were treated with Protein G-Sepharose (GE Healthcare,
234 Buckinghamshire, England) that had been previously incubated with rat anti-medaka Pgr
235 antibody, anti-medaka Creb1 antibody, anti-medaka Pik3cb antibody, anti-medaka Akt1
236 antibody, normal mouse IgG, normal rabbit IgG, or normal rat IgG. After incubation at 4
237 ºC for 16 h, the samples were washed with IP buffer three times, followed by two washes
238 with 50 mM Tris-HCl (pH 8.0). The precipitated materials were boiled in 1× SDS sample
239 buffer for 20 min and used for Western blot analysis. Normal IgGs served as a negative
240 control. The input was loaded with 2% of the extracts used for immunoprecipitation
241 experiments.
242
243 Western blot analysis was performed according to a previous method [36], except that an
244 ImmunoCruz^{TM} IP/WB Optima E System (Santa Cruz, Dallas, Texas) was used as a
245 dilution buffer for secondary antibodies. For detection of phosphoprotein, samples were
246 subjected to SDS-PAGE and transferred to a membrane. The membrane was blocked with

247 a blocking solution (1% BSA, 20 mM Tris-HCl (pH 7.5), 20 mM NaCl, 0.1% Tween 20,
248 0.02% NaN_3) for 1 h at room temperature and incubated with the primary antibody diluted
249 in the wash buffer (10 mM Tris-HCl (pH 7.5), 20 mM NaCl, 0.1% Tween 20) for 1 h.
250 After being washed with wash buffer three times, the membrane was incubated with
251 secondary antibody diluted in an ImmunoCruz^{TM} IP/WB Optima E System for 1 h. After
252 the membrane was washed with the wash buffer three times, signal was detected using an
253 Immobilon Western kit (Millipore, Bedford, MA). Detection of medaka Mmp15 [36] and
254 Pgr [34] proteins was performed as previously described. For detection of Rap1 protein,
255 Western blot analysis was performed according to a previously described method [36].
256 Rpl7 was used as a loading control. Antibody preincubated with the antigen (50 μg) in 50
257 mM Tris-HCl (pH 8.0) for 1 h at room temperature was used as the negative control. The
258 optical band density was measured with CS Analyzer 2.0 Software (ATTO, Tokyo, Japan).
259

260 ## Coimmunoprecipitation

261

262 Coimmunoprecipitation was performed as previously described [36], except that
263 preovulatory follicles 13 and 15 h before ovulation were used for the assay.
264

265 ## Preparation of primary granulosa cells (pGC)

266

267 pGC was prepared as previously described [44] expect that granulosa cells were isolated
268 from preovulatory follicles 14 h before ovulation.
269

270 ## Immunohistochemistry

271

272 Paraffin sections (5 μm thickness) were prepared as previously described [47]. The
273 sections were dewaxed in xylene for 5 min three times, placed in 99% ethanol for 2 min,
274 hydrated in a graded ethanol series, and rinsed in distilled water for 5 min. The specimens
275 were boiled in 10 mM sodium citrate (pH 6.0) for 45 min, washed with PBS for 5 min,
276 and incubated in PBS containing 3% H_2O_2 for 5 min. They were placed in PBS for 5 min
277 and then incubated in 10 mM Tris-HCl (pH 7.5), 0.15 M NaCl, 0.1% Tween, and 1% BSA
278 at room temperature for 60 min. The sections were reacted with anti-medaka Epac1
279 antibody diluted with PBS at room temperature for 60 min, washed with PBS for 20 min
280 three times, and incubated with Dako EnVision+System-HRP Labeled Polymer Anti-
281 mouse (Agilent Technologies, lnc. Santa Clara, CA) diluted with PBS at room
282 temperature for 60 min. After three 20-min washes with PBS, signals were detected using
283 an ImmPACT^{TM} AMEC Red Peroxidase Substrate kit (Vector Laboratories, Burlingame,
284 CA).

285

286 **Detection of active rap1**

287

288 Active medaka Rap1 was detected using a Rap Activation kit (Jena Bioscience, Jena,
289 Germany) according to the manufacturer's instructions. Briefly, preovulatory follicles (30
290 follicles per sample) were punctured with a needle and centrifuged at 1,500 g for 5 min.
291 The pellet was suspended gently in the lysis buffer supplied in the kit. The sample was
292 then centrifuged at 12,000 g for 15 min, and the resultant supernatant was incubated with
293 GST-RalGDS fusion protein and Glutathione-Resin. After 1 h of incubation, proteins
294 coupled with the Resin were recovered according to the method recommended by the

295 manufacturer. Active Rap1 was detected by Western blot analysis using commercially
296 available Rap1 antibody.
297
298 ## Chromatin immunoprecipitation (ChIP)
299
300 ChIP assay was performed as previously described [42], except that preovulatory follicles
301 (100 follicles per group) or follicles (120 follicles per group) cultured *in vitro* with or
302 without an inhibitor were used. Crosslinking, sonication, immunoprecipitation with
303 protein G-Sepharose-coupled medaka anti-Creb antibody, elution, reverse-crosslinking,
304 and RT-PCR were carried out as previously described [42]. Two sets of primers used for
305 PCR are given in Supplementary Information (Supplemental Table S1). Putative CREB
306 binding sites were searched using the free program TFBIND [48]. The site with a high
307 similarity (> 0.9) was selected as the putative binding site.
308
309 ## Establishment of a cell line stably expressing medaka Lh receptor (Lhr)
310 ## and Epac1
311
312 The coding region of Epac1 was amplified using KOD Fx DNA polymerase with the
313 pBlu-Epac1 as a template. The primer pair used was Epac1 pCMV-SS and Epac1 r-AS
314 (Supplemental Table S1). The PCR products were digested with *Eco*RI and *Xho*I, gel-
315 purified, and ligated into a pCMV tag4 vector (Agilent Technologies, Santa Clara, CA)
316 previously digested with the same enzymes. The resulting vector, pCMV-Epac1, was
317 digested with *Pci*I (New England BioLabs Inc., Ipswich, MA), and the overhangs were
318 filled in using Klenow Fragment (Takara, Osaka, Japan) to insert a hygromycin gene

under control of an SV40 promoter and a poly(A) signal. The gene cassette was amplified via PCR using pGloSensor-22F cAMP Plasmid (Promega, Madison, WI) as a template, KOD-Neo-DNA polymerase (Toyobo) and the primer pair Hyg-SS and Hyg-AS (Supplemental Table S1). The amplified product was phosphorylated, gel-purified, and ligated into the above pCMV-Epac1. The sequence of the resulting vector, pCMV-Epac1-Hyg, was confirmed by sequencing. Construction of pCMV-LHr, which was the vector carrying the medaka *lhr* gene, was performed as previously described [37]. Establishment of a cell line stably expressing medaka Lh receptor (Lhr) and Epac1 was carried out using a medaka caudal fin cell line (OLHNI-2) derived from HNI strain. The cell culture and cell transfection were performed according to previously reported methods [42]. pCMV-LHr was transfected into the cells, and the cells were incubated for 48 h. After incubation, the medium was changed to fresh medium containing 1 mg/ml G-418 (Wako). The cells were cultured for 14 more days, with medium changes every 2 days, followed by isolation and screening of single clones. The resulting cells stably expressing Lhr were further transfected with pCMV-Epac1. The transfection, selection, isolation and screening methods for single clones were the same as those described above, except that 0.5 mg/ml hygromycin B (Wako) was used for selection.

Knockout of *akt1* in OLHNI-2 cells expressing Lhr and Epac1

A Cas9 nuclease expression vector carrying a hygromycin B resistance gene (pCS2+hSpCas9/Hyg) was prepared as previously described [42]. The sgRNA expression vector was generated according to the previous method [42]. Briefly, the pair of oligonucleotides listed in Supplemental Table S1 was annealed and ligated into pDR274.

The resultant vector, pDR274-Akt1 was used for KO experiments. OLHNI-2 cells stably expressing Lhr and Epac1 using ScreenFect A (Wako) were cotransfected with pDR274-Akt1 and pCS2+hSpCas9/Hyg. After incubation for 48 h, the culture medium was exchanged with fresh medium containing 100 μg/ml hygromycin B (Wako), and cells were cultured for another 48 h. The cells were harvested and used for experiments.

Luciferase assay

A 1,335 or 1,084-bp nucleotide corresponding to a region that included the partial promoter and untranslated region of the *pgr* gene (−1119 to +216, or −868 to +216) was inserted into the pGL3 firefly luciferase expression vector (Promega Corporation, Madison, WI). OLHNI-2 cells stably expressing Lhr and Epac1 were transfected with pGL3-Pgr-1119-bp (−1119 to +216) or pGL3-Pgr-868-bp (−868 to +216) and with pRL, a Renilla luciferase expression vector (Promega Corporation), using ScreenFect A. After the cells were incubated in the presence or absence of rLh for 24 h, luciferase activity in the samples was measured using a Dual-Luciferase Reporter Assay System (Promega Corporation). Firefly luciferase activities were normalized to coexpressed Renilla luciferase activity.

Statistical analysis

All experiments were repeated 3 to 8 times. Error bars indicate the standard error of the mean (S.E.M.) obtained from 3 to 8 independent experiments. Statistical analysis of all data except for Figures 3E and 4E was conducted using one-way ANOVA followed by

Dunnett's post hoc test. Data for Figures 4E were analyzed by one-way ANOVA followed by Tukey's post hoc test, and data for Figure 3E were examined by Student's *t*-test. Equal variation was confirmed using an F-test or Bartlett's test, as appropriate. *P* values less than 0.05 (marked as *) or 0.01 (marked as **) were regarded as statistically significant. For RT-PCR, Western blot analysis, and immunohistochemistry, at least three separate experiments were performed to confirm the reproducibility of the findings, but the result of only one experiment is shown. For qRT-PCR and RT-PCR, cultured follicles (5 follicles per group) or preovulatory follicles (10 follicles per sample) isolated from two fish ovaries were used per experiment.

Results

Pgr and Mmp15 expression occur in a PKA-independent manner in preovulatory follicles after the LH surge

Preovulatory follicles isolated from the fish ovaries 22 h before ovulation were incubated *in vitro* with recombinant medaka Lh (rLh) in the presence or absence of various chemicals (Figure 1A). Follicles incubated with rLh successfully ovulated (Figure 1B). However, rLh-induced follicle ovulation was suppressed significantly when the follicles were incubated in the presence of MDL 12330A (adenylate cyclase inhibitor), H-89 (PKA inhibitor), brefeldin A (EPAC inhibitor), Wortmannin (PI3K/AKT antagonist), AKT inhibitor IV (AKT inhibitor), KG-501 (CREB inhibitor), or GGTI (RAP inhibitor). Next, we examined the expression of *pgr* and *mmp15* in preovulatory follicles or their follicle layers treated with these reagents. Except for H-89, treatment of the follicles with the

391 reagents resulted in significant inhibition of LH-induced *pgr*/Pgr (Figures 1C and 1E) and
392 *mmp15*/Mmp15 expression (Figures 1D and 1F) at both the mRNA and protein level. We
393 further examined the effects of other inhibitors on the expression of *pgr* in preovulatory
394 follicles. rLh-induced follicle expression of *pgr* was suppressed in a concentration-
395 dependent manner when the follicles were incubated in the presence of AC-V (adenylate
396 cyclase inhibitor), Epac-i (EPAC inhibitor), LY (PI3K inhibitor), AKT inhibitor-I (AKT
397 inhibitor), or CTEB-i (CREB inhibitor) (Supplemental Figure S2). The effects of other
398 inhibitors, an EGFR inhibitor, Salirasib (RAS inhibitor), U0126 (MEK inhibitor), and
399 PKC inhibitor, on ovulation and *pgr* expression in the follicles were also examined. These
400 four inhibitors also significantly reduced the rate of follicle ovulation, but none of them
401 showed an inhibitory effect on *pgr* expression in the follicle (Supplemental Figure S3).
402

403 **Epac1-Rap1 plays a role in mediating cAMP signaling to activate the**
404 **downstream pathway in preovulatory follicles after the LH surge**
405

406 We examined whether an exchange protein directly activated by cAMP (Epac) and the
407 downstream effector Rap are involved in the process of *pgr*/Pgr induction. Among the
408 three Epac and eight Rap genes known for medaka (Ensembl genome database,[49]), one
409 mRNA species of *rapgef3* (coding for Epac1) and two mRNA species of *rapgap1a*
410 (coding for Rap1a) and *rapgap1b1* (coding for Rap1b-1) were expressed in large
411 abundance (Supplemental Figure S4) in the ovary 17 h before ovulation, the time when
412 intracellular cAMP increased immediately after the LH surge.
413

414 Epac1 protein was localized in the oocyte cytoplasm of follicles with a diameter less than

100 μm, which were in the previtellogenic phase at stage I-III (Figure 2A, arrows). The protein was also expressed in the granulosa cells of follicles larger than 500 μm, which were in a late or post-vitellogenic phase at stage VIII-X (Figures 2A arrowheads and asterisk, 2C and 2D). No signal was observed in the section stained with absorbed antibody, indicating that the signal was specific (Figure 2B).

We next examined the expression and activation of Rap1a and Rap1b-1 in preovulatory follicles via Western blot analysis. The Rap1 antibody used in this study reacted with both medaka Rap1a and Rap1b-1 (Supplemental Figure S1B and C), and thus, we hereafter refer to the polypeptide detected with this antibody as Rap1 protein. Western blot analysis of the extracts prepared from preovulatory follicles in the first half (-23 to -11 h) of the 24 h spawning cycle revealed a single band of approximately 24 kDa (Figure 2E). The polypeptide band was steadily detected at all points of analysis, indicating constitutive expression in the follicles. Active Rap1 was detected using a GST-RalGDS pull-down assay. Active Rap1 was pulled-down by a GST-RalGDS fusion protein using extracts prepared from the preovulatory follicles and precipitated by Glutathione-Resins. The resulting precipitates were analyzed by Western blot using an anti-Rap 1 antibody (Figure 2F). Active Rap1 was also detectable at each point of analysis, but the greatest signal was detected significantly around -17 and-15 h (Figure 2G).

Activated Rap1 was detected in the follicles incubated for 3 h with rLh, but the rLh-induced activation of Rap1 was inhibited by brefeldin A (Figure 2H). Rap1 was also activated when the follicles were incubated with forskolin or 8-Br-cAMP, a cAMP analogue, in the absence of rLh (Figure 2I).

Activation of the PI3K-AKT pathway is a downstream event induced by Eapc1-Rap1 activated by the LH surge

We examined the possibility that the PI3K/AKT pathway may play a role in mediating EPAC1-RAP1 signaling to downstream pathways, eventually leading to *pgr*/Pgr expression.

PI3K is a heterodimer composed of a regulatory subunit and a catalytic subunit. Medaka possesses four genes for the catalytic subunit and five genes for the regulatory subunit. In this study, we examined the catalytic subunit of Pi3k for its expression in fish ovaries. qRT-PCR showed that three genes (*pik3c2a*, *Pik3c2b*, and *pik3c2g*) were expressed at detectable levels in the ovaries isolated 17 h before ovulation (Supplemental Figure S5), the time when follicles undergo the LH surge. On the other hand, among the four Akt genes (*akt1*, *akt2a*, *akt2b*, and *akt3* in official name) identified for medaka, the expression of *akt1* was the highest among in the -17 h ovary (Supplemental Figure S6).

Protein expression for the catalytic subunit of three Pi3k was examined by immunoprecipitation/Western blot analysis. Extracts prepared from preovulatory follicles were immunoprecipitated with each antibody and the resulting precipitates were examined by Western blot analysis. The analysis indicated that the Pi3k catalytic subunit, Pik3c2b (common name Pi3k-c2β), was only expressed at detectable levels in preovulatory follicles (Figure 3A, middle panel). We subsequently examined the possible involvement of Pi3k-c2β in the expression of *pgr*/Pgr. To determine whether Pi3k-c2β

463 interacts with active Rap1 in follicles that are destined to ovulate, active Rap1 was pulled-
464 down by a GST-RalGDS fusion protein using extracts isolated at various time points in
465 the first half of the 24 h-spawning cycle and precipitated by Glutathione-Resins. The
466 resulting Rap1 fraction was then analyzed by Western blotting using anti-medaka Pi3k-
467 c2β antibody. A clear band around -15 h of ovulation was detected significantly (Figure
468 3A, upper and lower panel), confirming an interaction between Rap1 and Pi3k-c2β around
469 this time in preovulatory follicles.
470
471 A steady expression of Akt1 in the preovulatory follicles was shown during the 24 h
472 spawning cycle (Figure 3B). However, an active phosphorylated form (pAkt1) of Akt1
473 was restrictedly detected significantly in the -19, -17 h, -15 h, -13 h, and -3 h-follicles
474 using antibody specific for phosphorylated ^{473}Ser, which is an active mark of Akt
475 activation and is required for its maximal activation [50, 51].
476
477 mTOR and PDK1 are known to be important protein kinases necessary for AKT
478 activation [51]. Constitutive expression of *mtor* and *pdk1* mRNA in the follicles
479 throughout the 24-h spawning cycle was confirmed by qRT-PCR (Supplemental Figure
480 S7), suggesting that Akt1 could be activated in preovulatory follicles.
481
482 Next, the effects of various inhibitors on Akt1 activation were investigated using -22 h-
483 follicles (Figure 3C). Incubation of the follicles with rLh for 3 h rapidly induced pAkt1
484 significantly. The rLh-induced phosphorylation of Akt1 was not inhibited by KG-501 or
485 H-89. However, Akt1 phosphorylation was suppressed by brefeldin A, Wortmannin, and
486 AKT inhibitor IV, suggesting the implication of activated EPAC and PI3K signaling in

the generation of pAkt1. To obtain further insights into the role of Akt1, we examined the induction of *pgr*/Pgr expression using a medaka OLHNI-2 cell line stably expressing both the medaka LH receptor (Lhcgr) and Epac1 (Rapgef3). In the cells cultured with medaka rLh, *pgr* expression was upregulated, but this *pgr* expression increase was abolished by the addition of AKT inhibitor IV (Figure 3D). Similar experiments were conducted using a cell line deficient in the *akt1* gene. The Akt1-knockout cells used were confirmed to express little or no Akt1 protein and it was estimated that over 80% of the cells were deficient in *akt1* (Figure 3E). rLh treatment of the control cells induced *pgr* expression, but the same treatment did not induce the expression of *pgr* in the *akt1*-deficient cells (Figure 3F). To confirm the reproducibility of the above finding, we also conducted experiments using single-guide RNA targeting a different *akt1* sequence (data not shown). The results of the two gene knockout approaches were basically the same, suggesting that the system achieved site-specific DNA recognition and cleavage of the target specifically. The results indicate that phosphorylated (active) Akt1 is involved in the expression of *pgr*.

Phosphorylated Creb1 functions as a transcription factor for expression of the *pgr* gene in preovulatory follicles

Medaka has two *creb* genes in the Ensembl genome database: *creb1* and *creb2*. We found that the ovaries of sexually mature medaka exclusively expressed the *creb1* gene (Supplemental Figure S8). Creb1 protein was detected in the preovulatory follicle throughout the 24-h spawning cycle (Figure 4A), but phosphorylated Creb1 was restrictedly detected around –23 h, –15 h, –13 h and –3 h of ovulation (Figure 4B and C). The expression of Pgr in preovulatory follicles was drastically induced at the same timing

511 (-15 h of ovulation) when phosphorylated Creb1 was detected.

512

513 We performed a promoter assay to examine the potential role of Creb1 in *pgr* expression
514 using OLHNI-2 cells stably expressing the medaka Lh receptor (Lhcgr) and Epac1
515 (Rapgef3). The cells were transfected with pGL3-Pgr-1119-bp or pGL3-Pgr -868-bp and
516 then treated with or without rLh. Luciferase activity was significantly increased when the
517 cells transfected with a vector containing the *pgr* promoter and a putative CREB binding
518 site were incubated with rLh (Figure 4D), indicating that the *cre* sequence in the promoter
519 of the medaka *pgr* gene is important for its transcription. Next, Creb1 binding to the *pgr*
520 promoter region was examined with a ChIP assay. Preovulatory follicles isolated at 23,
521 15, 10, and 4 h before ovulation were used for the assay. Creb1 recruitment to the
522 promoter was observed only with the -15 h-follicles (Figure 4E).

523

524 **Akt1 dominantly contributes to the Creb1 activation required for Lh-**
525 **induced follicular *pgr* expression**

526

527 To determine whether Akt1 may be implicated in the Creb1 activation necessary for *pgr*
528 expression in LH-stimulated preovulatory follicles, we first examined the possibility of
529 direct Akt1-Creb1 interaction in the follicle. Materials immunoprecipitated with anti-
530 medaka Akt1 antibody using extracts of the -15 h- and -13 h-follicles contained Creb1
531 (Figure 5A), indicating a direct interaction between Akt1 and Creb1 at the time when
532 activated Akt1 is formed in the follicles. Next, experiments were conducted using the cell
533 line stably expressing Lhr and Epac1 (Control) and the same cell line expressing Lhr and
534 Epac1 but not Akt1 (Akt1-KO). In the control cells, Creb1 was detected irrespective of

whether the cells were treated with rLh (Figure 5B, left panel), while active pCreb1(S133) was detected significantly in the rLh-treated cells. pCreb1(S133) was detectable if the control cells were incubated with H-89 or AKT inhibitor IV but was undetectable in cells incubated in the medium containing both H-89 and AKT inhibitor IV. In contrast, the pCreb1(S133) produced in Akt1-KO cells after incubation with rLh completely disappeared after the addition of H-89 in the culture medium (Figure 5B), indicating that the pCreb1(S133) found in Akt1-KO cells was due to the action of Pka. These results indicate that in addition to Pka, medaka Akt1 has the potential to phosphorylate Creb1 in cells, and this finding is consistent with previous reports stating that AKT could be an activator of CREB in mammalian species [52-54].

We further examined the relative contribution of Akt1 and Pka to the Creb1 activation required for *pgr* expression in Lh-stimulated follicles. When the -22 h-follicles were cultured with rLh, Creb1 was phosphorylated. Neither H-89 nor AKT inhibitor IV alone had an inhibitory effect on rLh-induced Creb1 phosphorylation in the follicles, but the phosphorylation reaction was strongly inhibited by the addition of both inhibitors (Figure 5C), which is consistent with the results of experiments using OLHNI2 cells (Figure 5B, left panel). The findings indicate that both Pka and Akt1 contribute to pCreb1 formation in LH-stimulated preovulatory follicles.

In the -22 h-follicles incubated with rLh for 3 h, pCreb1 was detected (Figure 5D). Further addition of KG-501, an inhibitor that interrupts formation of the CREB functional complex [55], to the culture did not affect Creb1 phosphorylation. ChIP assays were further conducted using primer pair-1 with the preovulatory follicles incubated with rLh

559 for 3 h. The follicles treated with rLh showed Creb1 recruitment to the *pgr* promoter, but
560 its recruitment was strongly inhibited by KG-501 (Figure 5E). In the -22 h-follicles
561 treated with rLh for 3 h, Creb1 binding to the promoter region of the *pgr* gene was
562 observed, but Creb1 binding was significantly reduced by the addition of AKT inhibitor
563 IV to the medium (Figure 5F). The above results confirm that pCreb1 is a transcription
564 factor required for expression of the *pgr* gene. The results also indicate the involvement
565 of Akt1 in Creb1 activation.
566
567 Finally, the localization and expression of the genes and/or proteins that may be involved
568 in the cAMP-EPAC-RAP-PI3k-AKT-CREB signaling pathway for Lh-induced *pgr*/Pgr
569 expression in medaka were examined in preovulatory follicles. Primary granulosa cells
570 isolated from the follicles obtained 14 h prior to ovulation expressed all the components
571 of the signaling pathway (Supplemental Figure S9), indicating that the proteins are
572 spatially and temporally associable in the cells.
573

574 # Discussion

575 In the present study, many inhibitors were used as blockers of target molecule(s) that were
576 suggested to be involved in the signaling pathway for the induction of medaka Pgr (Figure
577 1C). The outcomes of experiments using inhibitors need to be treated with caution to
578 determine whether they have specific inhibitory activity. In the present study, we found
579 that all inhibitors used inhibited the induction of *pgr* expression in a concentration-
580 dependent manner (Fig. S2). Furthermore, we examined whether the induction was
581 inhibited using two different blockers of cAMP, Epac, Rap, Pi3k, Akt, or Creb, and
582 treatment of preovulatory follicles with all inhibitors caused the inhibition of *pgr*

583 expression. Such a concentration-dependent inhibition and parallelism in the pattern of
584 effects on the follicles strongly argues that all blockers inhibit the target molecule(s).
585 However, our results do not completely rule out the potential toxicity and off-target effects
586 of the blockers at present.

587

588 Our present investigation provides evidence that the
589 cAMP/EPAC/RAP/PI3K/AKT/CREB signaling pathway is activated for LH-induced
590 induction of *pgr*/Pgr in preovulatory follicles at ovulation in the teleost medaka (Figure
591 6). Like other teleosts [56], both the theca and granulosa cells of preovulatory follicles
592 express Lh receptors in medaka [37]. However, existing evidence indicates that granulosa
593 cells play a principal role in ovulation with little, if any, contribution of theca cells to the
594 process [57, 58]. Therefore, in this model, the signaling pathway activated immediately
595 after the LH surge in the follicle is illustrated by focusing on the granulosa cell. Lh, which
596 is secreted from the pituitary gland approximately 17 h before ovulation in the 24-h
597 spawning cycle of the fish [37], binds to the Lh receptor expressed on granulosa cells,
598 resulting in synthesis of cAMP through adenylate cyclase activation [33]. The cAMP thus
599 synthesized binds to and activates Epac1. Activated Epac1 then turns on Rap1 by forming
600 the GTP-bound form of Rap1. Active Rap1 then activates the Pi3k-c2b/Akt1 pathway,
601 and the resulting active Akt1 phosphorylates Creb1 to generate the active form of the
602 transcription factor. Active Creb1 is recruited to the promoter region of *pgr* and drives its
603 expression. Judging from the timing of the occurrence of activated Rap1, active Akt1,
604 active Creb1, and active Creb1 binding to the *pgr* promoter region, the pathway becomes
605 active for a duration of only several hours (from -17 to -13 h, with a peak around -15 h)
606 in the granulosa cells of the follicles. This brief window of pathway activation is

607 necessary and sufficient to induce the rapid and transient expression of *pgr*/Pgr that
608 subsequently serves as a regulator of the expression of various ovulation-related
609 genes/proteins. It should be noted that Pgr is a progestin-activated transcription factor and
610 that progestins must be synthesized in the granulosa cells of the follicles in sufficient
611 quantities to activate Pgr. In medaka, 17α, 20β-dihydroxy-4-pregnen-3-one (17, 20βP) is
612 the naturally occurring progestin [56]. Activated Lh receptors on the granulosa cells of
613 preovulatory follicles upon the Lh surge induce a dramatic shift in the steroidogenic
614 pathway from estradiol-17β to 17,20βP, resulting in high follicular levels of 17,20βP [56].
615 Thus, the progestin readily binds to Pgr to induce activation when Pgr is synthesized in
616 the cells.
617
618 We found that Creb1 was phosphorylated by both Akt1 and Pka in the granulosa cells of
619 Lh-stimulated preovulatory follicles. This result indicates that, in addition to
620 cAMP/EPAC/RAP/PI3K/AKT/CREB signaling, the cAMP/PKA/CREB signaling
621 pathway is simultaneously activated in the follicles by the Lh surge. The involvement of
622 cAMP/PKA/CREB signaling in fish ovulation is evident from the current observation that
623 follicle ovulation was almost completely inhibited by H-89. Intriguingly, Akt inhibitor IV
624 strongly inhibited Creb1 binding to the *pgr* promoter region. In addition, all the inhibitors
625 affecting the EPAC/RAP/PI3K/AKT pathway substantially inhibited *pgr*/Pgr expression
626 in the treated follicles. However, the PKA inhibitor H-89 had no significant inhibitory
627 effect on follicular expression of *pgr*/Pgr. These findings indicate that active Creb1
628 generated by Akt1 may be preferably employed for transcription of the *pgr* gene in the
629 follicles (Figure 6). We should note our present observation that neither H-89 nor AKT
630 inhibitor IV alone had an inhibitory effect on rLh-induced Creb1 (Ser133)

phosphorylation in the follicles, but the phosphorylation reaction was strongly inhibited by the addition of both inhibitors. We presume that phosphorylated Creb1 could be simultaneously and independently produced through the cAMP/PKA and cAMP/EPAC/RAP/PI3K/AKT signaling pathways in the Lh-stimulated preovulatory follicle and that even one of these pathways was blocked by its respective inhibitor, the other pathway would still be active to produce phosphorylated Creb1. The generation of active Creb1 (Ser133) was completely suppressed only when the two inhibitors were added. Here, we question why Akt1-activated Creb1, but not Pka-activated Creb1, selectively contributes to the subsequent pgr transcription in the cytoplasm of granulosa cells. This could be explained by compartmentalization of signaling molecules and enzymes. Emerging evidence indicates that receptor signaling is restricted to highly organized compartments within the cell and that the functional confinement of signaling pathways provides a mechanism whereby the activation of distinct receptors provokes unique responses [59]. In the same way, signal compartmentalization in granulosa cells could be a cellular determinant that may facilitate the sole involvement of Akt1-activated Creb1 in the expression of pgr/Pgr. Alternatively, beyond the Ser133 of Creb1, an additional amino acid residue site(s) of the protein might be phosphorylated to function as a transcription factor for successful pgr expression, and only Akt1 could also phosphorylate the residue at the additional site. This might allow Akt1-activated Creb1 to participate in the pgr transcription event. In our present study, only the Ser133 phosphorylation status of Creb1 was analyzed and we have no information on the phosphorylation at other amino acid residues. Further studies are necessary to determine the exact mechanism by which active Creb1 is generated through the cAMP/EPAC/RAP/PI3K/AKT signaling pathway in the LH-stimulated preovulatory

655 follicle, together with the possibility of Pka involvement in this process. Nevertheless,
656 based on the current data, we tentatively assume that Akt-activated Creb1 mainly
657 participates in pgr induction.
658
659 Somewhat surprising is that although *pgr* transcription in the preovulatory follicles
660 appears to occur only for the several hours immediately following the Lh surge (from -17
661 to -13 h), *pgr*/Pgr are detected at high levels for a relatively long period of time (from -
662 15 to -7 h for *pgr* transcript and from -15 to -3 h for Pgr protein) in the 24 h-spawning
663 cycle of the fish [33, 34]. This indicates that rapidly transcribed *pgr* mRNA stably remains
664 in the granulosa cells of preovulatory follicles for a long period, even after the
665 transcription of *pgr* is terminated, ensuring that *pgr* mRNA is translated whenever the
666 transcription factor Pgr may be required for expression of ovulation-related genes. Our
667 previous studies revealed that expression of *ptger4b* (prostaglandin E_2 receptor subtype)
668 [33], *ccni* (cyclin I) [42], *pai1* (plasminogen activator inhibitor-1) [47, 58], and *mmp15*
669 [34], which are all ovulation-related genes in medaka, occurs in an Lh- and Pgr-dependent
670 manner. In the expression of these genes, the timing of Pgr binding to the promoter region
671 of the respective genes varies: -12 h for *pgtger4b*, -9 h for *ccni*, -6 h for *pai1*, and -4 h for
672 *mmp15*. At present, the mechanism by which *pgr* mRNA may be maintained without
673 degradation for a relatively long period of time in the granulosa cells of the follicles
674 undergoing ovulation is not known.
675
676 We believe that this study is the first report elucidating the entire signaling pathway
677 responsible for the expression of *pgr* in preovulatory follicles in vertebrates, especially
678 lower vertebrates, except mammals. Here, a question may be raised as to whether the

679 signaling pathway is unique for fish or conserved among other classes of vertebrates,
680 including mammals. Currently available data suggest the involvement of cAMP, PKA,
681 EGF-like peptides/EGFR, ERK1/2 and IP3/DAG in LH-induced follicular expression of
682 *Pgr*/PGR in mammals [15, 18-23]. Assuming that these signaling mediators play a central
683 role in follicular *Pgr* expression in mammals, the signaling pathway responsible for
684 follicular gene expression is quite different between mammals and medaka. Notably,
685 follicular *pgr* expression was not inhibited by respective inhibitors of the four kinases
686 EGFR, RAS, MEK, and PKC in the fish. This difference may be associated with the
687 distinct ovarian follicle structures. Here, we should note a recent study exploring the
688 signaling pathway associated with *PGR* expression in human uterine endometrial stromal
689 cells [60], which reports that hCG activates the ERK1/2 pathway through EPAC, causing
690 a transient increase in *PGR* transcripts and protein expression.
691
692 cAMP/PKA/CREB signaling also plays a critical role in medaka ovulation, as evidenced
693 by the strong suppression of rLh-induced follicle ovulation by H-89. It was reported in
694 mammals that the expression of some steroidogenic and related genes, such as
695 steroidogenic acute regulatory protein (StAR) and aromatase was regulated via the
696 cAMP/PKA/CREB pathway [61-64]. Iwamatsu and Shibata (2008) showed that forskolin
697 induced 17,20βP production in cultured medaka preovulatory follicles [65]. The findings
698 led the authors to speculate that some steroidogenic genes are regulated via the
699 cAMP/PKA/CREB pathway in medaka ovaries. The PI3K/AKT pathway is suggested to
700 be linked to the activation of RAS [66]. We observed in the present study that rLh-induced
701 follicle ovulation was strongly inhibited by the RAS inhibitor (Figure S3). It may be
702 possible that Ras activated via the Pi3k/Akt pathway is involved in medaka ovulation. In

addition, EGFR, RAS, MEK, and PKC protein kinase inhibitors were effective in inhibiting follicle ovulation. All of the above four inhibitors were without effect on LH-induced *pgr*/Pgr expression in preovulatory follicles. Future research into the specific roles of the above mediators would contribute greatly to overall understanding of the mechanisms that control ovulation in teleosts.

In summary, this is the first study in lower vertebrates to report the signal flow from the ovulatory surge of LH to eventual expression of the *pgr* gene in follicles destined for ovulation by demonstrating the role of each signaling component contributing to the pathway.

Conflicts of interest: The authors have no financial conflicts of interest to disclose concerning the study.

Author contributions:

K.O. designed the study, performed experiments, acquired and interpreted data and wrote the manuscript. M.H. designed the study, performed experiments, acquired and interpreted data. T.T. designed the study, interpreted data, and wrote the manuscript. All authors reviewed the manuscript and accepted the final version.

References

1. Lydon JP, DeMayo FJ, Funk CR, Mani SK, Hughes AR, Montgomery Jr. CA, Shyamala G, Conneely OM, O'Malley BW. Mice lacking progesterone receptor exhibit pleiotropic reproductive abnormalities. *Genes Dev* 1995; 9:2266-2278.

2. Petersen SL, Intlekofer KA, Moura-Conlon PJ, Brewer DN, Del Pino Sans J, Lopez JA. Novel progesterone receptors: neural localization and possible functions. *Front. Neurosci.* 2013; 7:164.

3. Shah, NM, Lai, PF, Imami, N, Johnson, MR. Progesterone-Related Immune Modulation of Pregnancy and Labor. *Front. Endocrinol.* 2019; 10:198.

4. Patel B, Elguero S, Thakore S, Dahoud W, Bedaiwy M, Mesiano S. Role of nuclear progesterone receptor isoforms in uterine pathology. *Hum Reprod Update* 2014; 21:155-173.

5. Bishop CV, Hennebold JD, Kahl CA, Stouffer RL. Knockdown of Progesterone receptor (PGR) in macaque granulosa cells disrupts ovulation and progesterone production. *Biol Reprod* 2016; 94(5): 109.

6. Zhu Y, Liu D, Shaner ZC, Chen S, Hong W, Stellwag EJ. Nuclear progestin receptor (pgr) knockouts in zebrafish demonstrate role for pgr in ovulation but not in rapid non-genomic steroid mediated meiosis resumption. *Front Endocrinol (Lausanne)* 2015; 6: 37.

7. Liu DT, Brewer MS, Chen S, Hong W, Zhu Y. Transcriptomic signatures for ovulation in vertebrates. *Gen Comp Endocrinol* 2017; 247: 74-86.

8. Akison LK, Robertson SA, Gonzalez MB, Richards JS, Smith CW, Russell DL, Robker RL. Regulation of the ovarian inflammatory response at ovulation by nuclear progesterone receptor. *Am J Reprod Immunol* 2018; 79(6): e12835.

9. Palanisamy GS, Cheon YP, Kim J, Kannan A, Li Q, Sato M, Mantena SR, Sitruk-Ware RL, Bagchi MK, Bagchi IC. A novel pathway involving progesterone receptor, endothelin-2, and endothelin receptor B controls ovulation in mice. *Mol Endocrinol* 2006; 20(11): 2784-95.

10. Park CJ, Lin PC, Zhou S, Barakat R, Bashir ST, Choi JM, Cacioppo JA, Oakley OR, Duffy DM, Lydon JP, Ko CJ. Progesterone receptor serves the ovary as a trigger of ovulation and a terminator of inflammation. *Cell Rep* 2020; 31(2): 107496.

11. Robker RL, Russell DL, Espey LL, Lydon JP, O'Malley BW, Richards JS. Progesterone-regulated genes in the ovulation process: ADAMTS-1 and cathepsin L proteases. *Proc Natl Acad Sci USA* 2000; 97:4689-4694.

12. Espey LL, Richards JS. Ovulation. In: Neill JD (eds.) *Physiology of Reproduction*, 3rd ed. Academic Press; 2006:425-474.

13. Kim J, Bagchi IC, Bagchi MK. Control of ovulation in mice by progesterone receptor-regulated gene networks. *Mol Hum Reprod* 2009; 15:821-828.

14. Robker RL, Akison LK, Russell DL. Control of oocyte release by progesterone

receptor-regulated gene expression. *Nucl Recept Signal* 2009; 7:e012.

15. Richards JS, Liu Z, Shimada M. Ovulation. In: Plant TM, Zeleznik AJ (eds.) *Physiology of Reproduction,* 4th ed. Academic Press; 2015:997-1021.

16. Choi Y, Rosewell KL, Brännström M, Akin JW, Curry TE, Jr. Jo M. FOS, a critical downstream mediator of PGR and EGF signaling necessary for ovulatory prostaglandins in the human ovary. *J Clin Endocrinol Metab* 2018; 103:4241-4252.

17. Dinh DT, Breen J, Akison LK, DeMayo FJ, Brown HM, Robker RL, Russell DL. Tissue-specific progesterone receptor-chromatin binding and the regulation of progesterone-dependent gene expression. *Sci Re.* 2019; 9:11966.

18. Park JY, Su YQ, Ariga M, Law E, Jin SLC, Conti M. EGF-like growth factors as mediators of LH action in the ovulatory follicle. *Science* 2004; 303:682-684.

19. Sekiguchi T, Mizutani T, Yamada K, Kajitani T, Yazawa T, Yoshino M, Miyamato K. Expression of epiregulin and amphiregulin in the rat ovary. *J Mol Endocrinol* 2004; 33:281-291.

20. Fan HY, Liu Z, Shimada M, Sterneck E, Johnson PF, Hedrich SM, Richards JS. MAPK3/1 in ovarian granulosa cells are essential for female fertility. *Science* 2009; 324:938-941.

21. Sayasith K, Lussier J, Doré M, Sirois J. Human chorionic gonadotropin-dependent up-regulation of epiregulin and amphiregulin in equine and bovine follicles during the ovulatory process. *Gen Comp Endocrinol* 2013; 180:39-47.

22. Prochazka R, Blaha M. Regulation of mitogen-activated protein kinase 2/1 activity during meiosis resumption in mammals. *J Reprod Dev* 2015; 61:495-502.

23. Richards JS, Ascoli M. Endocrine, Paracrine, and autocrine signaling pathways that regulate ovulation. Trends Endocrinol Metab 2018; 29(5): 313-325.

24. Parker M, Leonardsson G, White R, Steel J, Milligan S. Identification of RIP140 as a nuclear receptor cofactor with a role in female reproduction. *FEBS Lett* 2003; 546:149-153.

25. Breen SM, Andric N, Ping T, et al. Ovulation involves the luteinizing hormone-dependent activation of $G_{q/11}$ in granulosa cells. *Mol Endocrinol* 2013; 27:1483-1491.

26. Sriraman V, Sharma SC, Richards JS. Transactivation of the progesterone receptor gene in granulosa cells: Evidence that Sp1/Sp3 binding sites in the proximal promoter play a key role in luteinizing hormone inducibility. *Mol Endocrinol* 2003; 17:436-449.

27. Plant T. The hypothalamo-pituitary-gonadal axis. *J Endocrinol* 2015; 226:T41-54.

28. Kanda S. Evolution of the regulatory mechanisms for the hypothalamic-pituitary-gonadal axis in vertebrates-hypothesis from a comparative view. *Gen Comp*

826 *Endocrinol* 2019; 284:113075.
827
828 29. Schartl M. Beyond the zebrafish: diverse fish species for modeling human disease.
829 *Dis Model Mech* 2014; 7:181-192.
830
831 30. Jaenisch R, Bird A. Epigenetic regulation of gene expression: how the genome
832 integrates intrinsic and environmental signals. *Nat Genet* 2003; 33:245-254.
833
834 31. Lister AL, Van Der Kraak G, Rutherford R, MacLatchy D. *Fundulus heteroclitus*:
835 Ovarian reproductive physiology and the impact of environmental contaminants.
836 *Comp Biochem Physiol C Toxicol Pharmacol* 2011; 154:278-287.
837
838 32. Cavalieri V, Spinelli G. Environmental epigenetics in zebrafish. *Epigenetics*
839 *Chromatin* 2017; 10:46.
840
841 33. Hagiwara A, Ogiwara K, Katsu Y, Takahashi T. Luteinizing hormone-induced
842 expression of Ptger4b, a prostaglandin E2 receptor indispensable for ovulation of the
843 medaka *Oryzias latipes*, is regulated by a genomic mechanism involving nuclear
844 progestin receptor. *Biol Reprod* 2014; 90(6):126.
845
846 34. Ogiwara K, Takahashi T. Involvement of the nuclear progestin receptor in LH-
847 induced expression of membrane type 2-matrix metalloproteinase required for follicle
848 rupture during ovulation in the medaka. *Mol Cell Endocrinol* 2017; 450:54-63.
849
850 35. Liu DT, Carter NJ, Wu XJ, Hong WS, Chen SX, Zhu Y. Progestin and nuclear
851 progestin receptor are essential for upregulation of metalloproteinase in zebrafish

preovulatory follicles. *Front Endocrinol* 2018; 9:517.

36. Ogiwara K, Takano N, Shinohara M, Murakami M, Takahashi T. Gelatinase A and membrane-type matrix metalloproteinases 1 and 2 are responsible for follicle rupture during ovulation in the medaka. *Proc Natl Acad Sci USA* 2005; 102:8442-8447.

37. Ogiwara K, Fujimori C, Rajapakse S, Takahashi T. Characterization of luteinizing hormone and luteinizing hormone receptor and their indispensable role in the ovulatory process of the medaka. *PLoS ONE* 2013; 8:e54482.

38. de Rooij J, Zwartkruis FJT, Verheijen MHG, Cool RH, Nijiman SMB, Wittinghofer A, Bos JL. Epac is a Rap1 guanine-nucleotide-exchange factor directly activated by cyclic AMP. *Nature* 1998; 396:474-477.

39. Grandoch M, Roscioni S, Schmidt M. The role of Epac proteins, novel cAMP mediators, in the regulation of immune, lung and neuronal function. *Brit J Pharmacol* 2010; 159:265-284.

40. Schmidt M, Dekker FJ, Maarsingh H. Exchange protein directly activated by cAMP (epac): a multidomain cAMP mediator in the regulation of diverse biological functions. *Pharmacol Rev* 2013; 65:670-709.

41. Robichaux WG, Cheng X. Intracellular cAMP sensor EPAC: physiology, pathophysiology, and therapeutics development. *Physiol Rev* 2018; 98:919-1053.

42. Ogiwara K, Takahashi T. Nuclear progestin receptor phosphorylation by Cdk9 is required for the expression of Mmp15, a protease indispensable for ovulation in medaka. *cells* 2019; 8:215.

43. National Center for Biotechnology Information (NCBI) database. NCBI, Bethesda, MD.http://www.ncbi.nlm.nih.gov/. Accessed August 1,2020.

44. Ogiwara K, Takahashi T. A dual role of melatonin in medaka ovulation: Ensuring prostaglandin synthesis and actin cytoskeleton rearrangement in follicle cells. *Biol. Reprod* 2016; 94(3):64.

45. Ogiwara K, Takahashi T. Specificity of the medaka enteropeptidase serine protease and its usefulness as a biotechnological tool for fusion-protein cleavage. *Proc Natl Acad Sci USA* 2007; 104:7021-7026.

46. Ogiwara K, Minagawa K, Takano N, Kageyama T, Takahashi T. Apparent involvement of plasmin in early-stage of follicle rupture during ovulation in medaka. *Biol Reprod* 2012; 86(4):113.

47. Ogiwara K, Hagiwara A, Rajapakse R, Takahashi T. The role of urokinase plasminogen activator and plasminogen activator inhibitor-1 in follicle rupture during ovulation in the teleost medaka. *Biol Reprod* 2015; 92(1):10.

48. TFBIND Tsunoda T: Medical Science Mathematics, RIKEN Center. http://tfbind.hgc.jp/ Accessed August 1,2020.

902
903 49. Ensembl database. The Wellcome Trust Genome Campus, Hinxton, U. K.
904 http://uswest.ensembl.org/index.html. Accessed August 1,2020.
905
906 50. Manning BD, Toker A. AKT/PKB Signaling: Navigating the Network. *Cell* 2017;
907 169:381-405.
908
909 51. Sarbassov DD, Guertin DA, Ali SM, Sabatini DM. Phosphorylation and regulation
910 of Akt/PKB by the rictor-mTOR complex. *Science* 2005; 307:1098-1101.
911
912 52. Du K, Montminy M. CREB is a regulatory target for the protein kinase Akt/PKB. *J*
913 *Biol Chem* 1998; 273:32377-32379.
914
915 53. Pugazhenthi S, Nesterova A, Sable C, et al. Akt/protein kinase B up-regulate Bcl-2
916 expression through cAMP-response element-binding protein. *J Biol Chem* 2000;
917 275:10761-10766.
918
919 54. Herkel J, Schrader J, Erez N, Lohse AW, Cohen IR. Activation of the Akt-CREB
920 signalling axis by a proline-rich heptapeptide confers resistance to stress-induced cell
921 death and inflammation. *Immunology* 2017; 151:474-480.
922
923 55. Best JL, Amezcua CA, Mayr B, Flechner LL, Murawsky CM, Emerson B, Zor T,
924 Gardner KH. Identification of small-molecule antagonists that inhibit an activator:
925 coactivator interaction. *Proc Natl Acad Sci USA* 2004; 101:17622-17627.
926
927 56. Nagahama Y, Yamashita M. Regulation of oocyte maturation in fish. *Dev Growth*

928 *Differ* 2008; 50:S195-219.
929
930 57. Takahashi T, Hagiwara A, Ogiwara K. Prostaglandins in teleost ovulation: A review
931 of the roles with a view to comparison with prostaglandins in mammalian ovulation.
932 *Mol Cell Endocrinol* 2017; 461:236-247.
933
934 58. Takahashi T, Hagiwara A, Ogiwara K. Follicle rupture during ovulation with an
935 emphasis on recent progress in fish models. *Reproduction* 2019; 157:R1-R13.
936
937 59. Ellisdon AM, Halls ML. Compartmentalization of GPCR signaling controls unique
938 cellular responses. *Biochem Soc Trans* 2016; 44(2):562-567.
939
940 60. Tapia-Pizarro A, Archiles S, Angandoña F, Vakebcua C, Zavaketa J, Johnson MC,
941 González-Ramos R, Devoto L. hCG activates Epac-Erk1/2 signaling regulating
942 protesterone receptor expression and function in human endometrial stromal cells.
943 *Mol Hum Reprod* 2017; 23:393-405.
944
945 61. Fitzpatrick SL, Richards JS. Identification of a cyclic adenosine 3′, 5′-
946 monophosphate-response element in the rat aromatase promoter that is required for
947 transcriptional activation in rat granulosa cells and R2C leydig cells. *Mol Endocrinol*
948 1994; 8:1309-1319.
949
950 62. Michael MD, Michael LF, Simpson ER. A CRE-like sequence that binds CREB and
951 contributes to cAMP-dependent regulation of the proximal promoter of the human
952 aromatase P450 (CYP19) gene. *Mol Cell Endocrinol* 1997; 134:147-156.
953

63. Arakane F, King SR, Du Y, et al. Phosphorylation of steroidogenic acute regulatory protein (StAR) modulates its steroidogenic activity. *J Biol Chem* 1997; 272:32656-32662.

64. Manna PR, Dyson MT, Eubank DW, et al. Regulation of steroidogenesis and the steroidogenic acute regulatory protein by a member of the cAMP response-element binding protein family. *Mol Endocrinol* 2002; 16:184-199.

65. Iwamastu T, Shibata Y. Effects of Inhibitors on Forskolin- and Testosterone-Induced Steroid Production by Preovulatory Medaka Follicles. *Bulletin Aichi Univ Edu* 2008; 57:73-79.

66. Ramjaun AR, Downward J. Ras and phosphoinositide 3-kinase: partners in development and tumorigenesis. *Cell Cycle* 2007; 6(23):2902–2905.

Figure legends

Figure 1. Effects of various inhibitors on the induction of *pgr*/Pgr and *mmp15*/Mmp15 expression and ovulation in preovulatory follicles. (A) An outline of preovulatory follicle culture experiments. Follicles isolated from spawning medaka ovaries 22 h before ovulation (-22 h-follicles) were cultured in the presence of recombinant medaka Lh (rLh) with or without various inhibitors. The expected timing of the Lh surge, GVBD, and ovulation *in vivo* and *in vitro* are shown. After 12 h or 30 h of incubation, the follicles or the follicle layers of the follicles were collected for analysis. (B) The -22 h-follicles were

cultured in the presence of rLh with the indicated inhibitor and the ovulation rates were determined after 30 h of incubation. **P<0.01 (ANOVA and Dunnett's post hoc test, N=6). (C and D) The -22 h-follicles were cultured as in (B) for 12 h (for *pgr*) or 30 h (for *mmp15*), and follicular expression of *pgr* (C) and *mmp15* (D) mRNA was determined by qRT-PCR. The expression levels were normalized to those of *eef1a* and expressed as the fold-change compared with the levels in follicles cultured without inhibitor (None). **P<0.01 (ANOVA and Dunnett's post hoc test, N=6). (E and F) The -22 h-follicles were cultured as in (B) for 12 h (for Pgr) or 30 h (for Mmp15), and follicular expression of Pgr (E) and Mmp15 protein (F) was detected by Western blot analysis. The dotted line represents cropping of a single gel. The signal intensity of the Pgr (E) or Mmp15 (F) band was quantified densitometrically, and the ratio of expression of Pgr or Mmp15 to Rpl7 was determined as the relative expression (each lower panel). An asterisk indicates a significant difference at $P < 0.05$ (*) or $P < 0.01$ (**) compared with the intensity in follicles cultured without inhibitor (None). (one-way ANOVA, post hoc Dunnett test, n = 4).

Figure 2. Follicular expression of Epac1 and *rap1*/Rap1 and *in vitro* Rap1 activation. (A and B) Immunohistochemistry was conducted for the -17 h-ovary using anti-Epac1 antibody (A) or anti-Epac1 antibody previously treated with recombinant Epac1 (B). Arrows indicate small follicles less than 100 μm, and arrowheads indicate growing follicles larger than 500 μm. An asterisk indicates a fully grown follicle for ovulation. (C) The boxed area in (A) is enlarged. (D) The boxed area in (C) is further enlarged. TC, theca cell; GC, granulosa cell; OM, oocyte membrane. Scale bars indicate 0.5 mm in (A) and (B), and 0.05 mm in (C). (E) Rap1 was detected in extracts of preovulatory follicles

isolated from ovaries at the indicated time points. As a negative control, the extract of the -15 h-follicles was processed in parallel using normal mouse IgG. Signals for Rap1 (arrow) and bands corresponding to the antibody used for immunoprecipitation (asterisk) are shown. (F) Active Rap1 was detected in extracts of preovulatory follicles prepared at the indicated time points. As a negative control, extract of the -15 h-follicles boiled for 10 min was used. Signals for active Rap1 (arrow) and bands corresponding to the Ral-GST used for the assay (asterisks) are shown. The dotted line represents cropping of a single gel. (G) The signal intensity of the active Rap1 band was quantified densitometrically, and the ratio of expression of active Rap1 to total Rap1 was determined as the relative expression. An asterisk indicates a significant difference at $P < 0.05$ (*) compared with the intensity at -23 h. (one-way ANOVA, post hoc Dunnett test, $n = 4$). (H) The -22 h-follicles were cultured with no additives, with rLh or with both rLh and brefeldin A for 3 h and then used to detect active Rap1. As a control, total Rap1 protein was detected using the input fractions. (H) The -22 h-follicles were cultured alone, with forskolin or with cAMP for 3 h, and then used to detect active Rap1. As a control, total Rap1 protein was detected using the input fractions. The signal intensity of the active Rap1 band was quantified densitometrically, and the ratio of expression of active Rap1 to total Rap1 was determined as the relative expression (each right panel). An asterisk indicates a significant difference at $P < 0.01$ (**) compared with the intensity in follicles cultured without rLh (-rLH in (H)) or chemical (None in (I)). (one-way ANOVA, post hoc Dunnett test, $n = 4$).

Figure 3. Follicular expression of Pi3k-c2β, Akt1, and pAkt1 and the effects of inhibitors on Akt1 activation. (A) In the upper panel, proteins containing active Rap1 were obtained

through a GST-RalGDS fusion protein and Glutathione-Resin, with follicle extracts and analyzed by Western blot analysis using anti-medaka Pi3k-c2b antibody. As a negative control, the extract of -15 h-follicles boiled for 10 min was used. In the middle panel, Pik3-c2b was detected by immunoprecipitation/Western blot analysis. As a negative control, the extract of -15 h follicles was immunoprecipitated using normal mouse IgG bound to protein G-Sepharose. The signal intensity of the Pi3k-c2b band was quantified densitometrically, and the ratio of expression of Pi3k-c2b (upper panel) to Pi3k-c2b (middle panel) was determined as the relative expression (lower panel). An asterisk indicates a significant difference at $P < 0.05$ (*) or $P < 0.01$ (**) compared with the intensity at -23 h. (one-way ANOVA, post hoc Dunnett test, $n = 4$). (B) pAkt1 (upper panel) and Akt1 (middle panel) were detected in follicle extracts via immunoprecipitation/Western blot analysis. As a negative control, the extract of -17 h-follicles was immunoprecipitated using normal mouse IgG bound to protein G-Sepharose. The lower panel shows the detection of Rpl7 protein using the input fractions as a control. The dotted line represents cropping of a single gel. (C) The -22 h-follicles were cultured in the presence of rLh with inhibitors for 3 h, and the extracts were analyzed for pAKt1 (upper panel) and Akt1 (lower panel) expression using immunoprecipitation/Western blot analysis. The signal intensity of the pAkt1 band was quantified densitometrically, and the ratio of expression of pAkt1 to total Akt was determined as the relative expression (each lower panel). An asterisk indicates a significant difference at $P < 0.05$ (*) or $P < 0.01$ (**) compared with the intensity at -23 h (B) or in follicles cultured without rLh (Cont in (C)). (one-way ANOVA, post hoc Dunnett test, $n = 4$). (D) OLHNI-2 cells stably expressing medaka Lhr and Epac1 were cultured for 12 h in the presence or absence of rLh with or without AKT inhibitor IV, and the resulting cell extracts were subjected to qRT-PCR for

detection of *pgr* mRNA expression. The expression levels were normalized to those of *eef1a*. *P<0.05 (ANOVA and Dunnett's post hoc test, N=6). (E) The expression of Akt1 protein in extracts of OLHNI-2 cells stably expressing medaka Lhr and Epac1 (Cont) and cells deficient for the *akt1* gene (Akt1-KO) was detected by Western blot analysis. Rpl7 was used as a control. The signal intensity of the Akt1 band was quantified densitometrically, and the ratio of expression of Akt1 to Rpl7 was determined as the relative expression (right panel). An asterisk indicates a significant difference at $P < 0.01$ (**) compared with the intensity at -23 h (B) or in follicles cultured without rLh (Cont in (C)). (Student's *t*-test, n = 4). (F) The control and Akt1-KO cells in (E) were cultured with or without rLh. After 12 h of incubation, qRT-PCR detection of *pgr* mRNA was conducted. The expression levels were normalized to those of *eef1a*. *P<0.05 (ANOVA and Dunnett's post hoc test, N=6).

Figure 4. Detection of Creb1 and pCreb1 in preovulatory follicles and binding of Creb1 to the *pgr* gene promoter. (A and B) Creb1 (A), pCreb1 (upper panel in B) and Pgr (lower panel in B) were detected in follicle extracts via immunoprecipitation/Western blot analysis. As a negative control, the extract of -15 h-follicles was immunoprecipitated using normal mouse IgG bound to protein G-Sepharose. The arrow indicates Creb1/pCreb1, and the asterisk denotes the band corresponding to the antibody used for immunoprecipitation. The dotted line represents cropping of a single gel. (C) The signal intensity of the pCreb1 band was quantified densitometrically, and the ratio of expression of pCreb1(A) to total Creb1 (B) was determined as the relative expression. An asterisk indicates a significant difference at $P < 0.05$ (*) or $P < 0.01$ (**) compared with the intensity at -21 h (one-way ANOVA, post hoc Dunnett test, n = 4). (D) A promoter assay

was conducted using OLHNI-2 cells stably expressing medaka Lhr and Epac1. The cells were transiently cotransfected with pGL3-Pgr-1119-bp with three putative CREB binding sites or pGL3-Pgr-868-bp without the sites. After 24 h of incubation with or without rLh, luciferase activity was measured. *P<0.05 (ANOVA and Dunnett's post hoc test, N=6). UTR, untranslated region; Luc, luciferase. (E) Preovulatory follicles isolated at the indicated time points were used for a ChIP assay using primer pair-1. As a negative control, the assay was performed with -15 h-follicles using primer pair-2. The upper panel illustrates the positions of the two ChIP primer pairs used, the putative CRE response element, and the TATA box in the upstream region of the transcription start site (indicated as +1) of the *pgr* gene. **P<0.01 (ANOVA and Tukey's post hoc test, N=6).

Figure 5. Creb1 phosphorylation by Akt1 and its role as a transcription factor in LH-induced follicular expression of the *pgr* gene. (A) Extracts of -13 h- and -15 h-follicles (for experiments) and -15 h-follicles (for control) were immunoprecipitated using an Akt1 antibody or normal IgG, and the precipitates were analyzed via Western blot using anti-Creb1 antibody (upper panel) and anti-Akt1antibody (lower panel). The signal intensity of the Creb1 band was quantified densitometrically, and the ratio of expression of Creb1 to Akt1 was determined as the relative expression. (B) OLHNI2 cells stably expressing medaka Lhr and Epac1 (left panel) and OLHNI2 cells stably expressing medaka Lhr and Epac1 but lacking medaka Akt1 (right panel) were incubated for 3 h with the inhibitors indicated. After incubation, pCreb1 (upper panel) and Creb1 (lower panel) were detected via immunoprecipitation/Western blot analysis. (C) The -22 h-follicles were cultured for 3 h with the inhibitors indicated in the presence or absence of rLh and the resulting cell extracts were analyzed for pCreb1 (upper panel) and Creb1 (lower panel) expression via

immunoprecipitation/Western blot analysis. The dotted line represents cropping of a single gel. (D) The -22 h-follicles were cultured for 3 h with or without KG-501 in the presence or absence of rLh, and the resulting cell extracts were analyzed for pCreb1 (upper panel) and Creb1 (lower panel) expression via immunoprecipitation/Western blot analysis. As a negative control for immunoprecipitation, the extract of follicles cultured with rLh for 3 h was immunoprecipitated using normal mouse IgG bound to protein G-Sepharose. The dotted line represents cropping of a single gel. The signal intensity of the pCreb1 band was quantified densitometrically, and the ratio of expression of pCreb1 to total Creb was determined as the relative expression. An asterisk indicates a significant difference at $P < 0.05$ (*) or $P < 0.01$ (**) compared with the intensity in follicles cultured without rLh (Cont in (B and C)) or KG-501 (D) (one-way ANOVA, post hoc Dunnett test, n = 4). (E and F) The -22 h-follicles were cultured for 3 h with or without KG-501 (E) or AKT inhibitor IV (F) and in the presence or absence of rLh. After incubation, a ChIP assay was conducted using primer pair-1 as in Fig. 4D. $^{**}P<0.01$ compared with the enrichments of the follicles cultured without rLh (ANOVA and Dunnett's post hoc test, N=6).

Figure 6. A model of the signaling pathway that induces Pgr expression in medaka preovulatory follicles after the LH surge. For details, see the text.

Figure 1

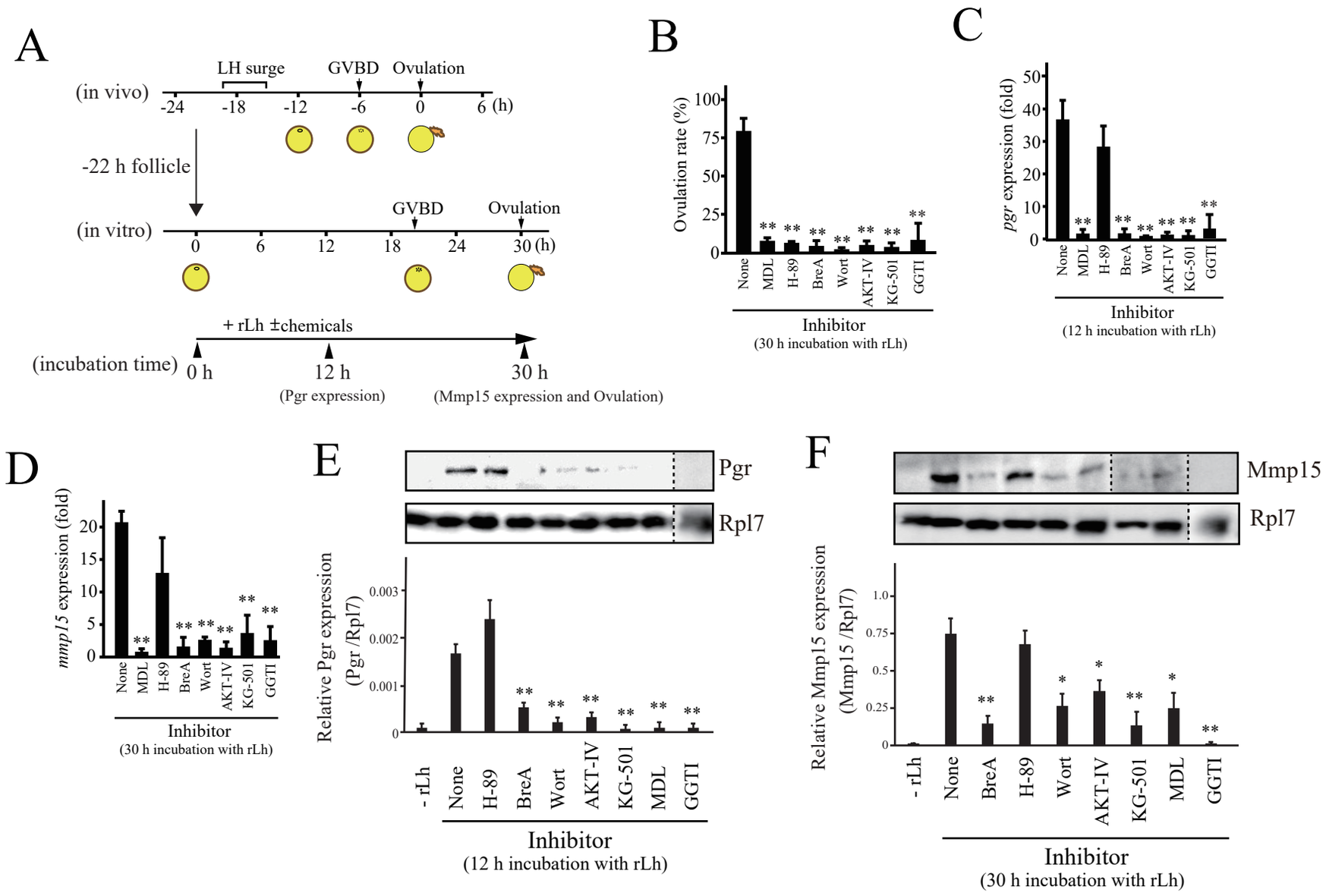
A
LH surge
GVBD
Ovulation
(in vivo)
-24
-18
-12
-6
0
6 (h)
-22 h follicle
GVBD
Ovulation
(in vitro)
0
6
12
18
24
30 (h)
+ rLh ±chemicals
(incubation time)
0 h
12 h
(Pgr expression)
30 h
(Mmp15 expression and Ovulation)
B
Ovulation rate (%)
None
MDL
H-89
BreA
Wort
AKT-IV
KG-501
GGTI
Inhibitor
(30 h incubation with rLh)
C
pgr expression (fold)
Inhibitor
(12 h incubation with rLh)
D
mmp15 expression (fold)
Inhibitor
(30 h incubation with rLh)
E
Pgr
Rpl7
Relative Pgr expression
(Pgr /Rpl7)
- rLh
Inhibitor
(12 h incubation with rLh)
F
Mmp15
Rpl7
Relative Mmp15 expression
(Mmp15 /Rpl7)
Inhibitor
(30 h incubation with rLh)

Figure 2

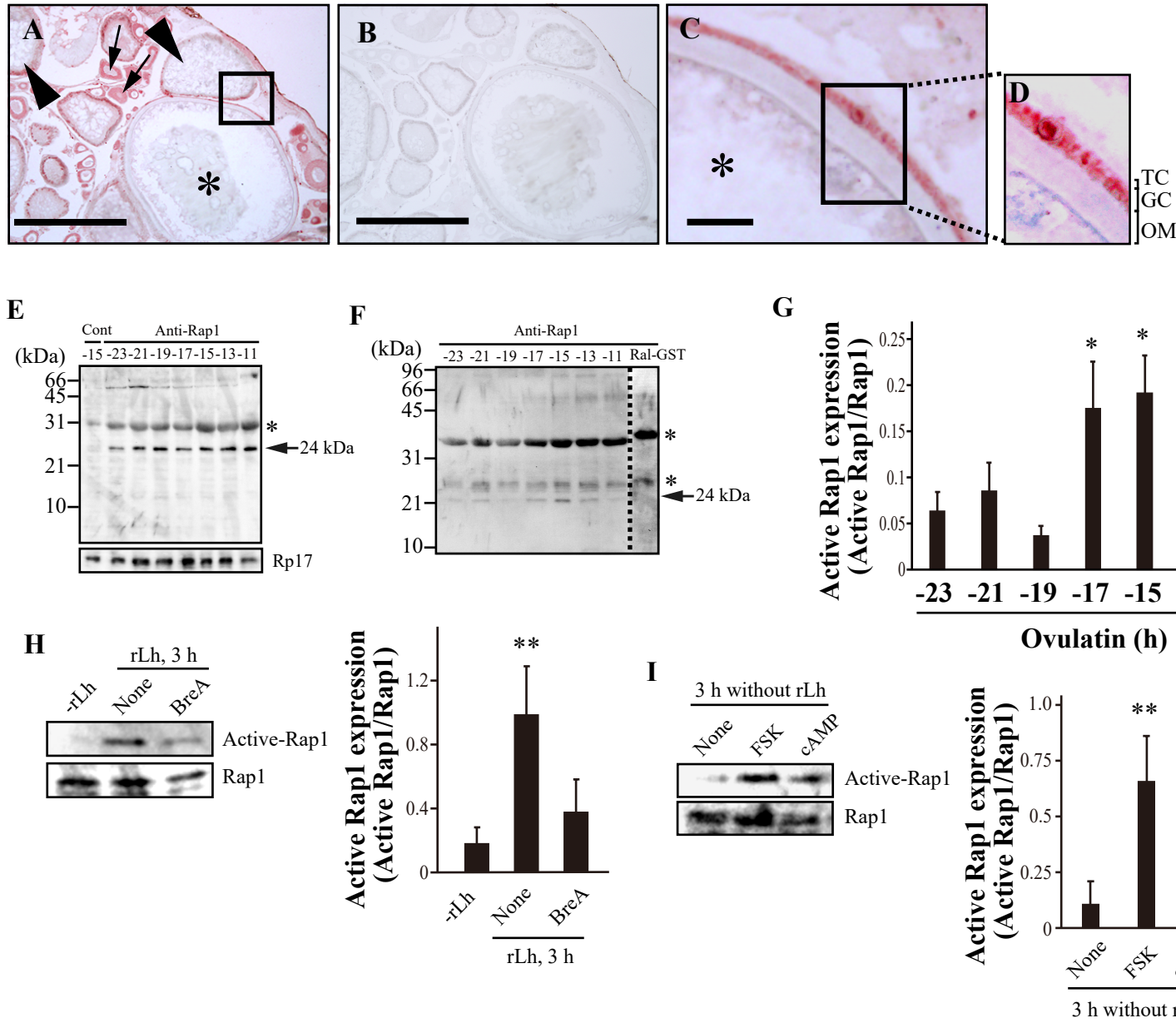
A
B
C
D
TC
GC
OM
E
Cont
Anti-Rap1
(kDa)
-15 -23 -21 -19 -17 -15 -13 -11
66
45
31
21
10
24 kDa
Rp17
F
Anti-Rap1
(kDa)
-23 -21 -19 -17 -15 -13 -11 Ral-GST
96
66
45
31
21
10
24 kDa
G
Active Rap1 expression
(Active Rap1/Rap1)
0.25
0.2
0.15
0.1
0.05
0
-23 -21 -19 -17 -15 -13 -11
Ovulatin (h)
H
rLh, 3 h
-rLh
None
BreA
Active-Rap1
Rap1
Active Rap1 expression
(Active Rap1/Rap1)
1.2
0.8
0.4
0
-rLh
None
BreA
rLh, 3 h
I
3 h without rLh
None
FSK
cAMP
Active-Rap1
Rap1
Active Rap1 expression
(Active Rap1/Rap1)
1.0
0.75
0.5
0.25
0
None
FSK
cAMP
3 h without rLh

Figure 3

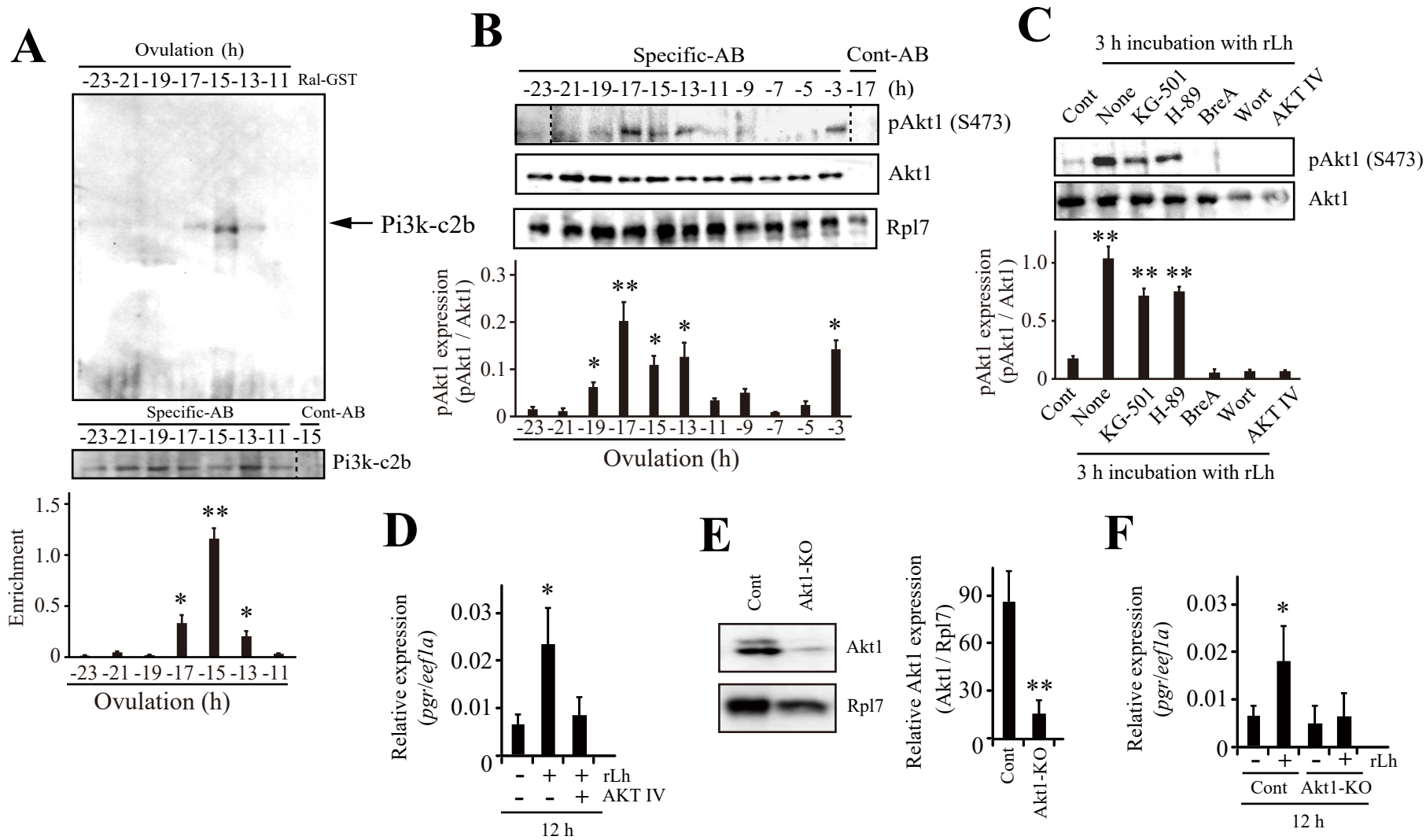
A
Ovulation (h)
-23-21-19-17-15-13-11 Ral-GST
Pi3k-c2b
Specific-AB
Cont-AB
-23-21-19-17-15-13-11 -15
Pi3k-c2b
Enrichment
Ovulation (h)
B
Specific-AB
Cont-AB
-23-21-19-17-15-13-11 -9 -7 -5 -3 -17 (h)
pAkt1 (S473)
Akt1
Rpl7
pAkt1 expression (pAkt1 / Akt1)
Ovulation (h)
C
3 h incubation with rLh
Cont None KG-501 H-89 BreA Wort AKT IV
pAkt1 (S473)
Akt1
pAkt1 expression (pAkt1 / Akt1)
3 h incubation with rLh
D
Relative expression (pgr/eef1a)
rLh
AKT IV
12 h
E
Cont Akt1-KO
Akt1
Rpl7
Relative Akt1 expression (Akt1 / Rpl7)
F
Relative expression (pgr/eef1a)
rLh
Cont Akt1-KO
12 h

Figure 4

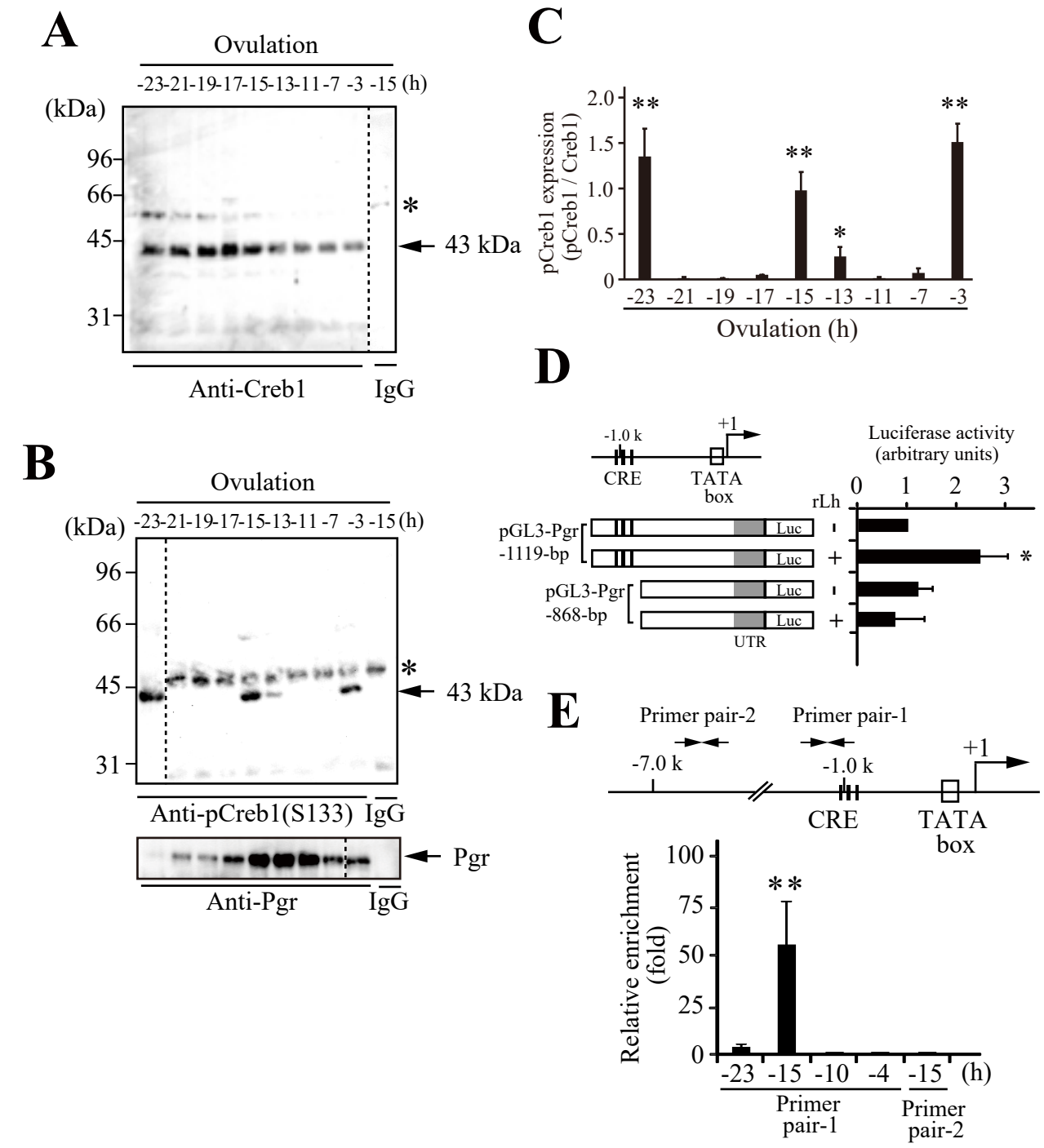
A
Ovulation
-23-21-19-17-15-13-11-7 -3 -15 (h)
(kDa)
96
66
45
31
*
43 kDa
Anti-Creb1
IgG
B
Ovulation
(kDa) -23-21-19-17-15-13-11-7 -3 -15 (h)
96
66
45
31
*
43 kDa
Anti-pCreb1(S133) IgG
Pgr
Anti-Pgr
IgG
C
pCreb1 expression
(pCreb1 / Creb1)
2.0
1.5
1.0
0.5
0
**
**
*
**
-23 -21 -19 -17 -15 -13 -11 -7 -3
Ovulation (h)
D
-1.0 k
+1
CRE
TATA
box
Luciferase activity
(arbitrary units)
0 1 2 3
rLh
pGL3-Pgr
-1119-bp
Luc
+
*
pGL3-Pgr
-868-bp
Luc
+
UTR
E
Primer pair-2
Primer pair-1
-7.0 k
-1.0 k
+1
CRE
TATA
box
Relative enrichment
(fold)
100
75
50
25
0
**
-23 -15 -10 -4 -15 (h)
Primer
pair-1
Primer
pair-2

Figure 5

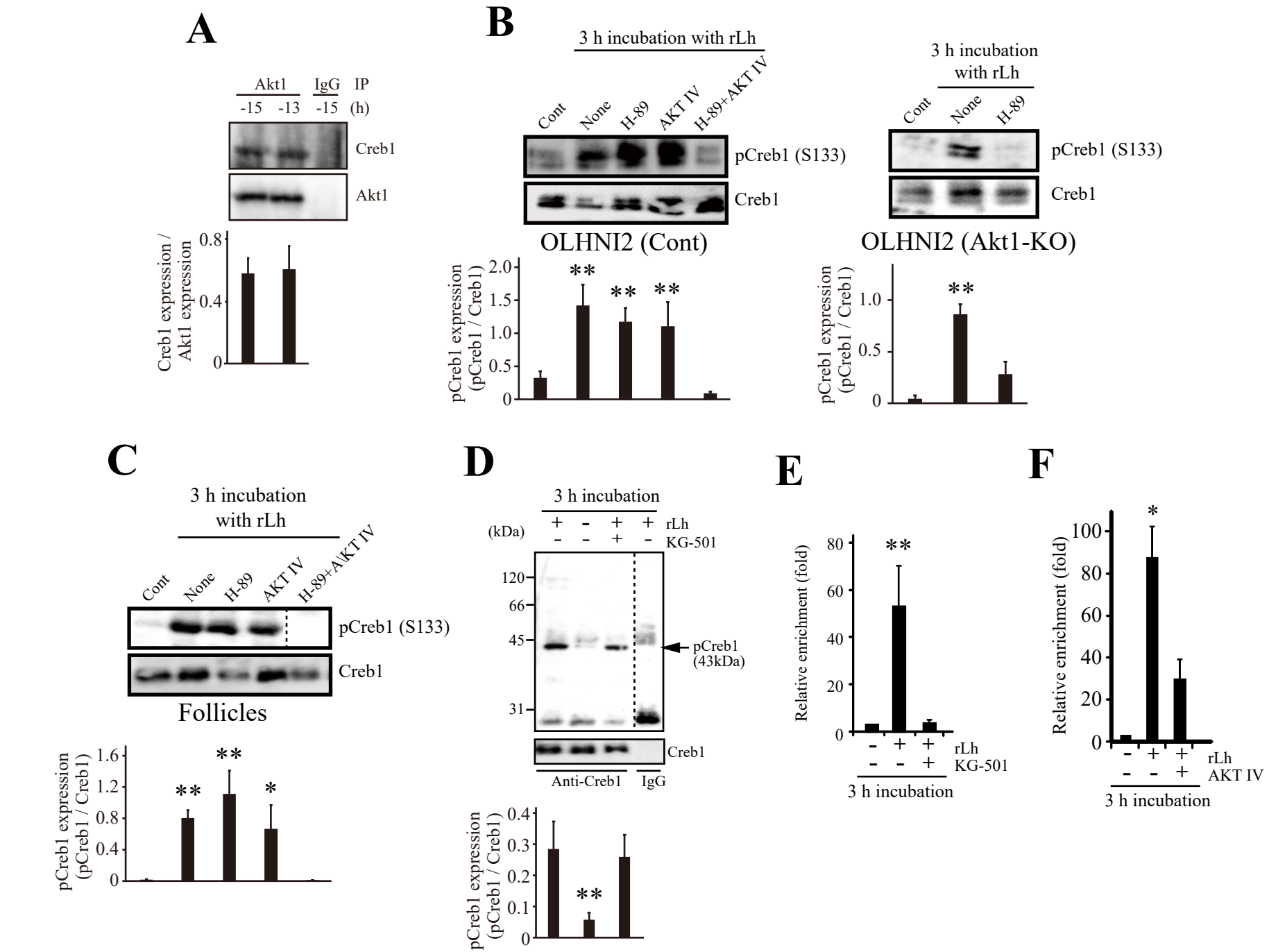
A
Akt1
IgG
IP
-15
-13
-15
(h)
Creb1
Akt1
Creb1 expression / Akt1 expression
B
3 h incubation with rLh
Cont
None
H-89
AKT IV
H-89+AKT IV
pCreb1 (S133)
Creb1
OLHNI2 (Cont)
pCreb1 expression (pCreb1 / Creb1)
3 h incubation with rLh
Cont
None
H-89
pCreb1 (S133)
Creb1
OLHNI2 (Akt1-KO)
pCreb1 expression (pCreb1 / Creb1)
C
3 h incubation with rLh
Cont
None
H-89
AKT IV
H-89+AKT IV
pCreb1 (S133)
Creb1
Follicles
pCreb1 expression (pCreb1 / Creb1)
D
3 h incubation
(kDa)
rLh
KG-501
120
66
45
31
pCreb1 (43kDa)
Creb1
Anti-Creb1
IgG
pCreb1 expression (pCreb1 / Creb1)
E
Relative enrichment (fold)
rLh
KG-501
3 h incubation
F
Relative enrichment (fold)
rLh
AKT IV
3 h incubation

Figure 6

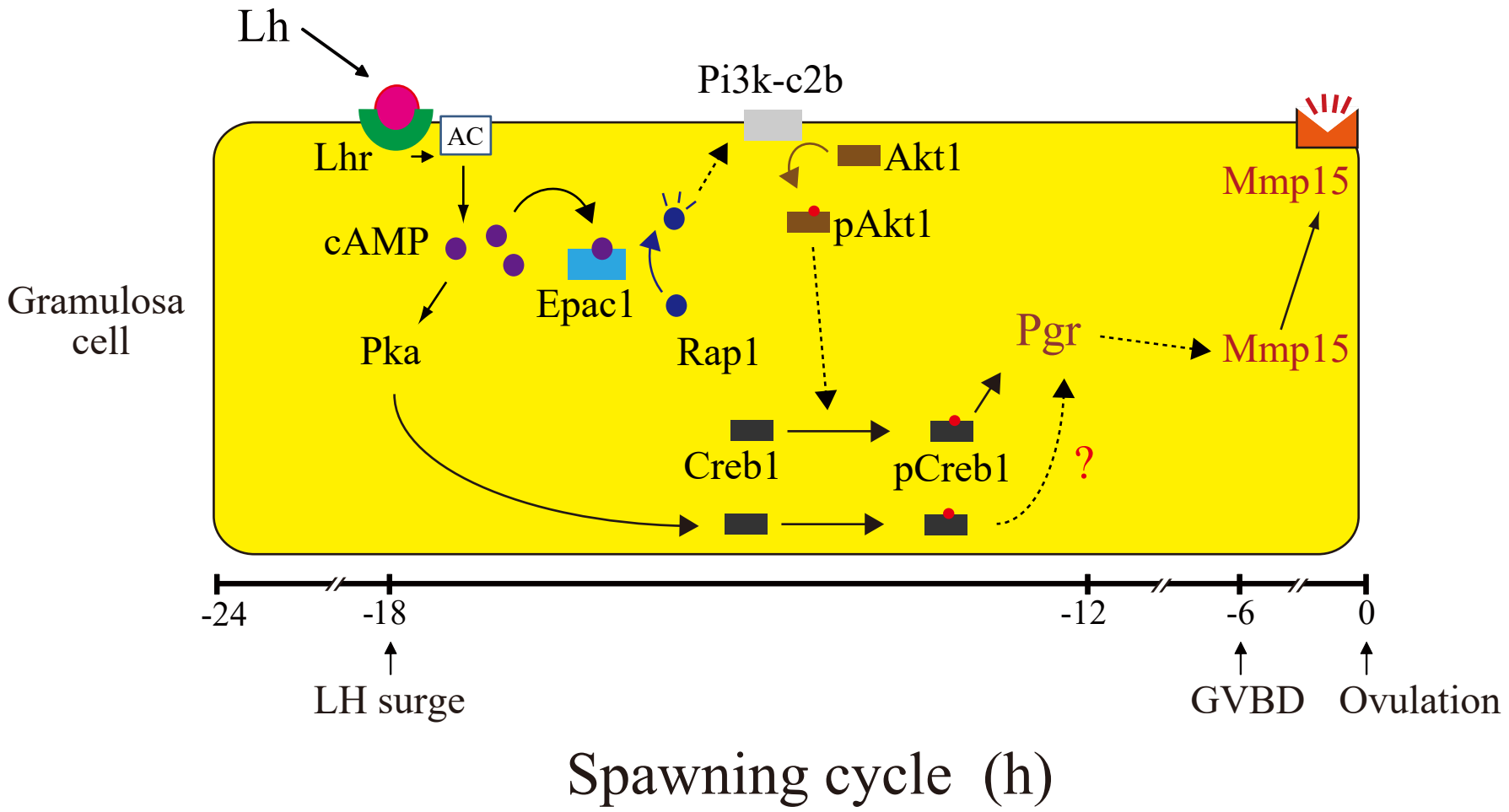
Lh
Pi3k-c2b
Lhr
AC
Akt1
Mmp15
cAMP
pAkt1
Gramulosa cell
Epac1
Rap1
Pka
Pgr
Mmp15
Creb1
pCreb1
?
-24
-18
-12
-6
0
LH surge
GVBD
Ovulation
Spawning cycle (h)

Supplemental Figure S1

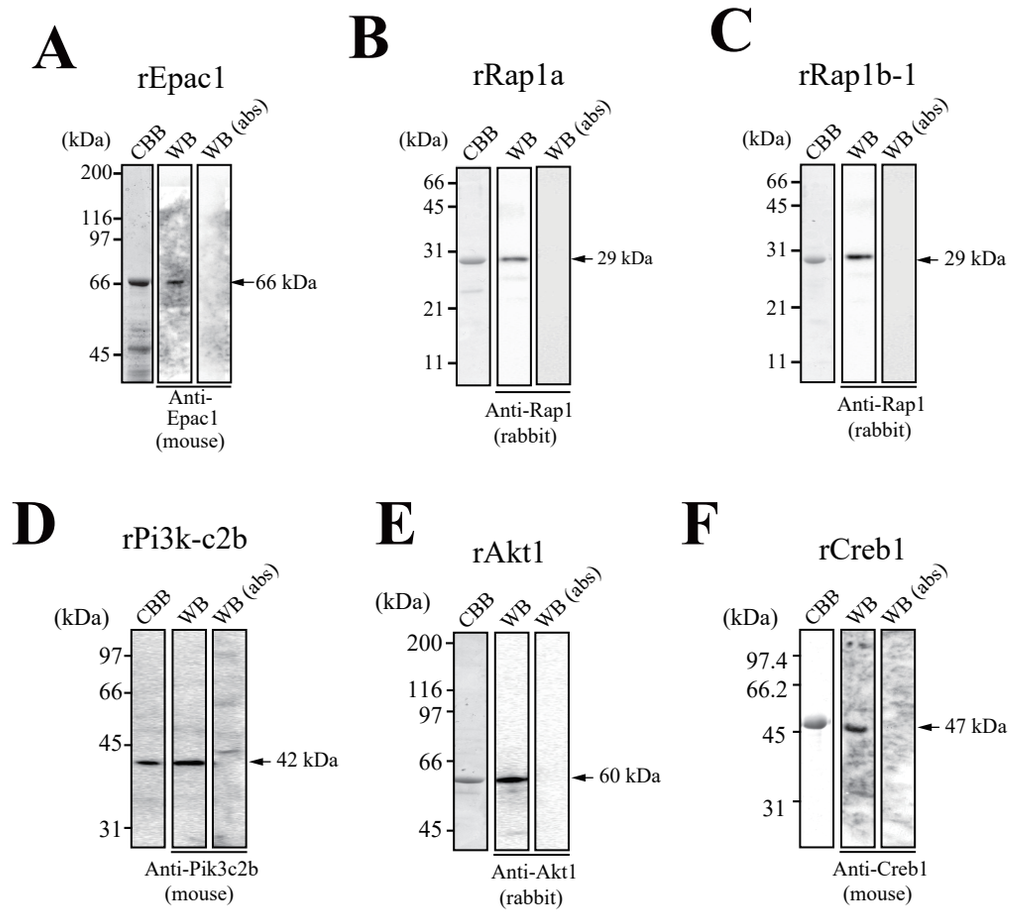

Supplemental Figure S2

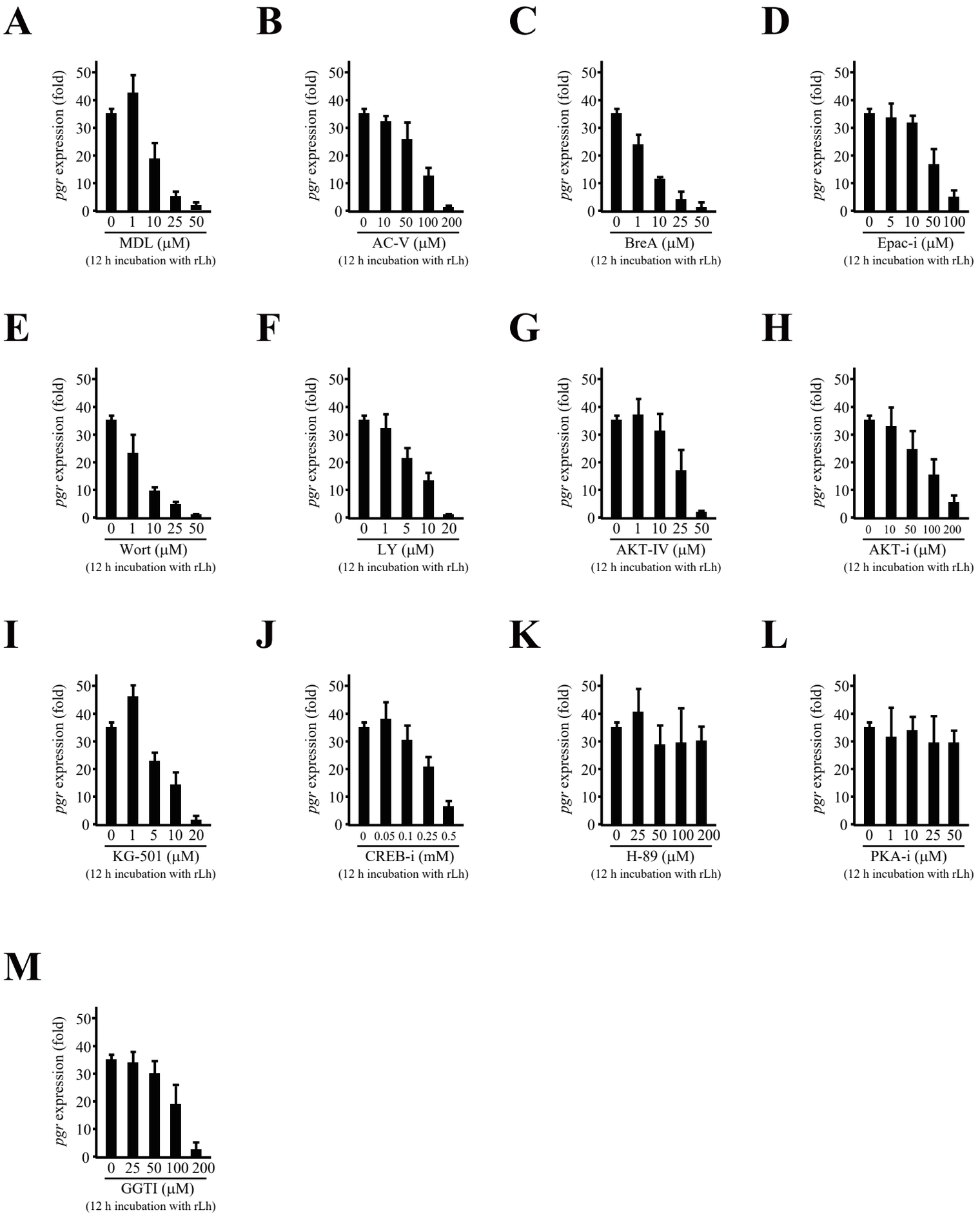

Supplemental Figure S3

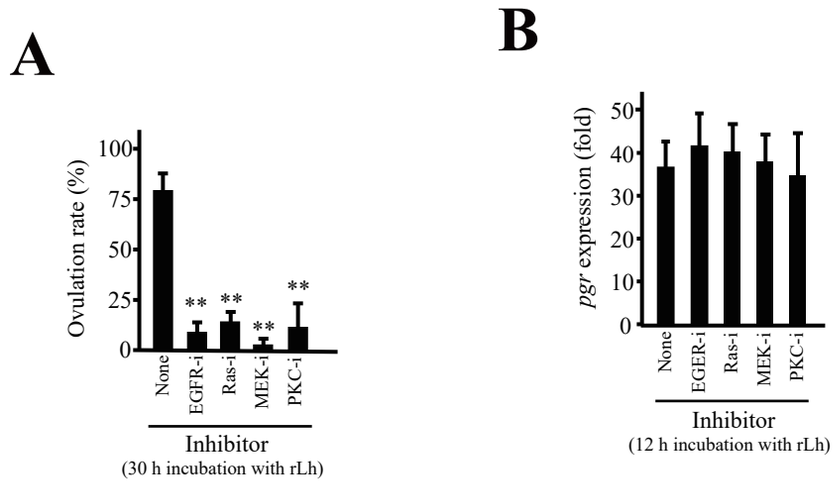

Supplemental Figure S4

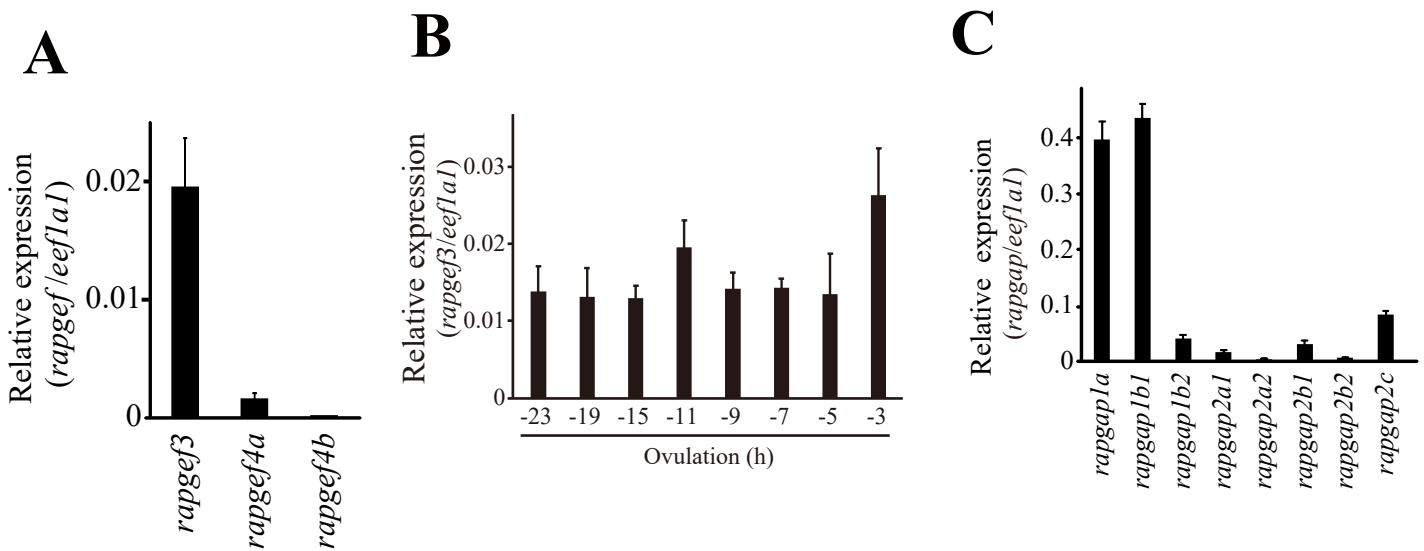

Supplemental Figure S5

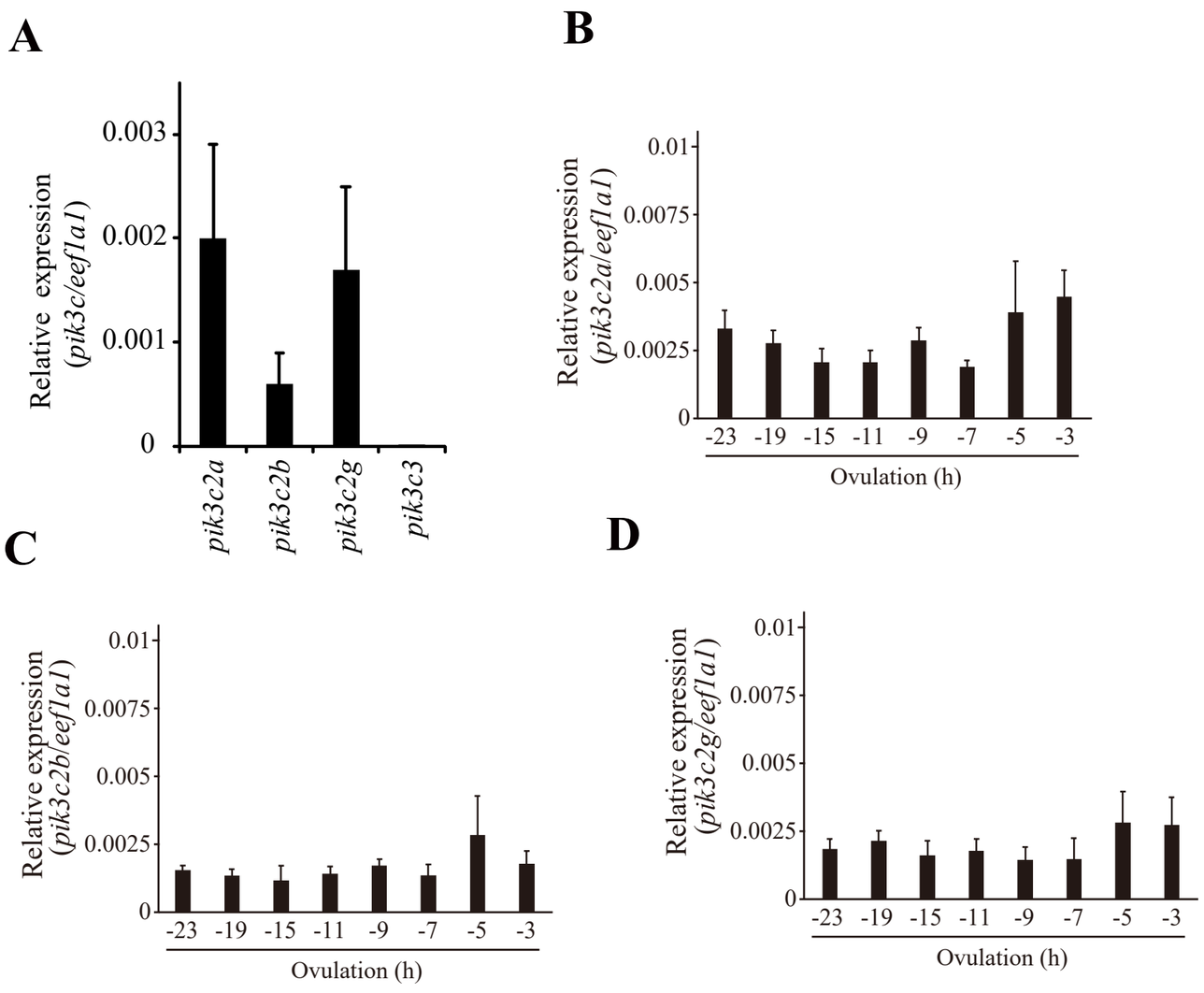

Supplemental Figure S6

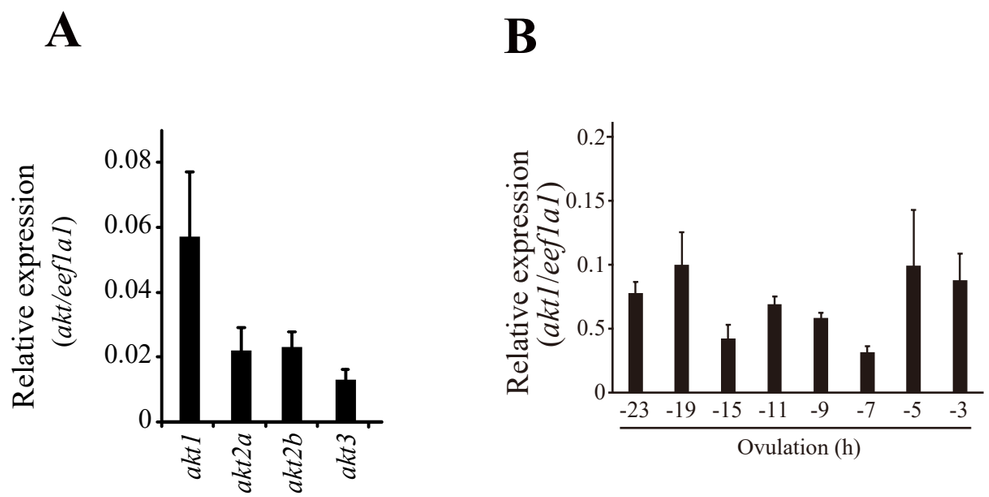

Supplemental Figure S7

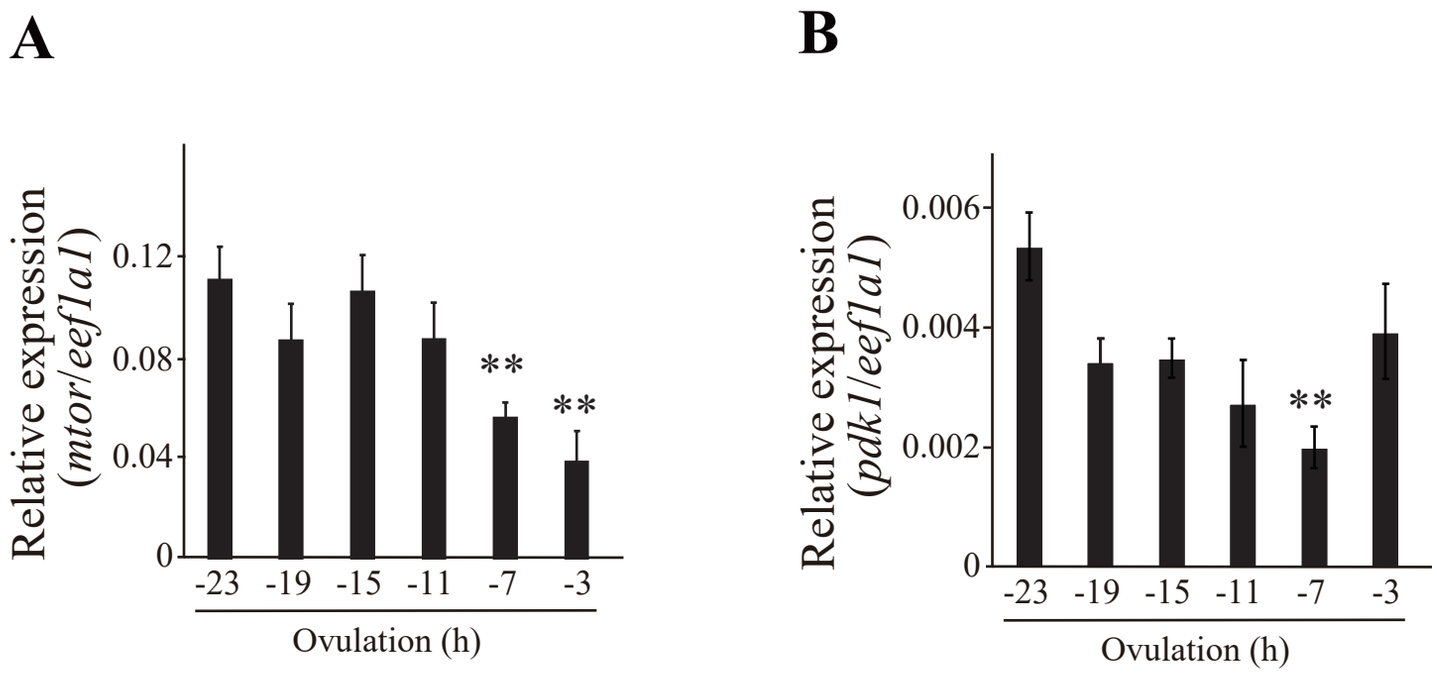

Supplemental Figure S8

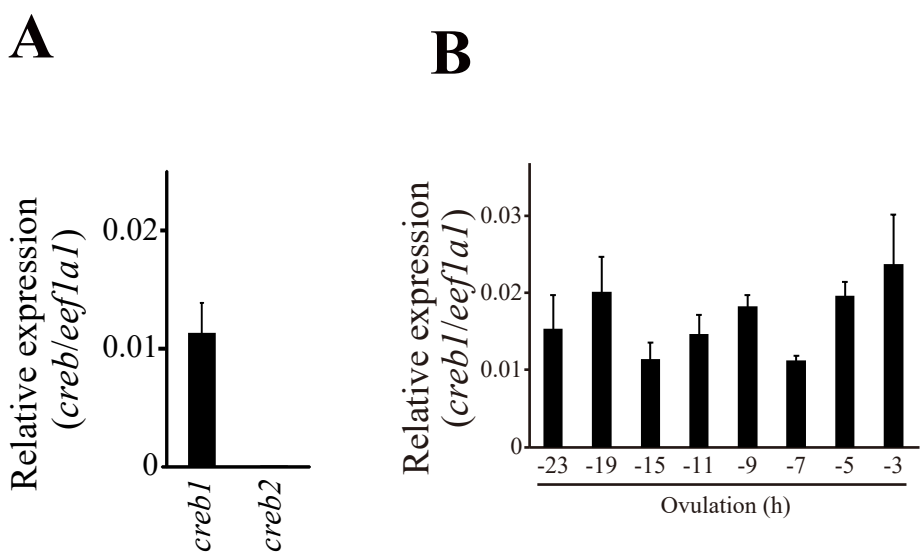

Supplemental Figure S9